10-2014

Shear Inducing Device for the Testing of Cell Fragility

Ramnath Raghunathan

SHEAR INDUCING DEVICE FOR THE TESTING OF CELL FRAGILITY

By

Ramnath Raghunathan

A thesis presented in partial fulfillment of requirement for the degree of

Master of Science in Mechanical Engineering

Approved by

Dr. Steven W. Day, PhD_____
Department of Mechanical Engineering (Thesis Advisor)

Dr. Hany Ghoneim, PhD_____
Department of Mechanical Engineering

Dr. Kathleen Lamkin-Kennard, PhD _____
Department of Mechanical Engineering

Dr. Mark Olles, PhD _____
Department of Manufacturing and Mechanical Engineering Technology

Rochester Institute of Technology
Kate Gleason College of Engineering
Department of Mechanical Engineering
Rochester, NY
October 2014

Acknowledgment

Foremost, I would like to express my gratitude to my advisor Dr. Steven Day for the continuous support, inspiration, guidance, patience and vast knowledge of my Masters Research. I also thank him for giving me the opportunity and the freedom to work with the blood pump and blood.

Besides my advisor, I would like to thank the rest of my thesis committee: Dr. Hany Ghoneim, Dr. Kathleen Lamkin-Kennard and Dr. Mark Olles for their encouragement, support, and insightful comments.

I want to thank the faculty of the Mechanical Department: William Finch, Diane Selleck, Robert Kraynik, Jan Maneti, Jill Ehmann and Michelle Horan of the Biomedical Engineering Department for their timely help and guidance. I also thank my fellow lab mates and friends: Brian Vanger, Shehan Jayasekara, Sarah Stoltzfus, Aishwarya Ganapathy Subramaniam and Kasturi Chandwadkar.

Last but not least, I would like to thank my family: Ramamurthi Raghunathan (Father), Kamala Raghunathan (Mother) and Divya Raghunathan (Sister) for their love and support.

This work was partially supported through the FDA Critical Path Initiative project on "Improving the use of Computational Fluid Dynamics Modeling to Predict Blood Damage Safety in Medical Devices", and that the Maglev test model was designed and developed through a joint FDA-RIT collaboration.

Abstract

Most blood pumps are designed to boost the pumping abilities of the heart by mechanical energy transfer using a rotor. Due to the nature of blood contacting devices, the various components of blood are subjected to shear stresses caused by the device. The accurate analysis and prediction of blood damage during the design phase of a device has been difficult to achieve. This has been complicated by both the inaccuracy of computer tools used to model the blood flow and the large uncertainty in the reported values of stress that damage blood components. Different components of blood, such as red blood cells, platelets and VWF (Von Willebrand Factor), have different sensitivities to shear stress. Further, the damage to blood components has been correlated to both the magnitude of the shear stress and duration of time that the components are exposed to that stress (exposure time). A device that is based on cylindrical Couette flow was developed by Rochester Institute of Technology called the Maglev (Magnetic Levitation) shearing device. This device has a magnetically suspended rotor thus reducing a major amount of friction when compared to pumps with bearings. The device is intended to have a single region of laminar Couette flow (between an inner rotating cylinder and a stationary housing) that exposes the fluid to stress. From prior work, the device was partially manufactured but never made to work. The two primary goals of this thesis are to fabricate a functional magnetically levitated shearing device to induce stress in blood and other fluids using the new fluid path design and to determine the damage done to bovine blood at different exposure and stress levels.

Table of Contents

List of Figures

List of Tables

Symbols and Acronyms

RIT - Rochester Institute of Technology

CFD - Computational fluid dynamics

LVAD - Left Ventricular Assist Device

HESA - Hall Effect Sensor Arrays

AMB – Active Magnetic Bearings

RBC - Red Blood Cells

F_{XP} – Front positive X direction AMB

F_{YP} – Front positive Y direction AMB

F_{XN} – Front negative X direction AMB

F_{YN} – Front negative Y direction AMB

R_{XP} – Rear positive X direction AMB

R_{YP} – Rear positive Y direction AMB

R_{XN} – Rear negative X direction AMB

R_{YN} – Rear negative Y direction AMB

HF_{XP} – Front positive X direction HESA

HF_{YP} – Front positive Y direction HESA

HF_{XN} – Front negative X direction HESA

HF_{YN} – Front negative Y direction HESA

HR_{XP} – Rear positive X direction HESA

HR_{YP} – Rear positive Y direction HESA

HR_{XN} – Rear negative X direction HESA

HR_{YN} – Rear negative Y direction HESA

I.H - Index of Hemolysis or Hemolysis Index

DC - Direct Current

Hz – Hertz

I.H – Index of Hemolysis

ms - millisecond

min - minute

sec - second

V - Volt

cP - Centipoises

μm - Micrometer

nm - nanometer

Pa - Pascal

τ - Shear stress

Δt - Exposure time

D – Shear damage

fHb – Free Hemoglobin in blood

tHb – Total Hemoglobin in blood

R – Radius of the rotor

L – Shear gap height

d – Shear gap width

N – Speed of the rotor

Q – Volumetric flow rate

μ - Viscosity of blood

1 INTRODUCTION

Artificial Organs in direct contact with the blood stream are generally associated with flow induced blood damage[1]. Blood pumps, like most artificial organs, are required to satisfy high demands on functionality and biocompatibility. The term functionality means that the function of the pump must be similar to that of the heart itself and biocompatibility means the artificial organ needs to be adaptable with the human body and its organs. Most artificial organs are prone to post implant complications, such as mechanical failure of diaphragms and valves or the material of construction is not suitable for the body. Over the years, a definite link between fluid shear-induced damage and activation of blood constituents such as platelets and red blood cells (RBC) has been established[2]. The time factor, known as exposure time, and stress levels play an important role in blood damage. The best way to determine the blood damage caused by any mechanical assisted pump is to analyze the motion of the pump and its effect on the blood flowing through it.

The two major types of blood damage that can occur are thrombosis and hemolysis[3]. Hemolysis is the breakage of the RBC membrane, causing the release of hemoglobin and other internal components into the surrounding fluid. Thrombosis is the formation of a blood clot inside a blood vessel, obstructing the flow of blood through the circulatory system. Thrombosis is a series of events, but can be initiated by the mechanical activation of platelets resulting from fluid mechanical shear stress. Flow properties such as high shear stress and stagnation are believed to be the major cause of hemolytic and thrombus formation. The most quantitative method of correlation between the shear stress and exposure time is the power law model[4] (Equation 1).

$$D = A\tau^{\alpha}\Delta t^{\beta} \quad \textbf{(1)}$$

where D represents the rate of generation of plasma free hemoglobin, τ represents the shear stress RBC is exposed to, and Δt represents the time duration. A, α, and β are obtained from the regression of experimental data. This study will experimentally determine hemolysis values by exposing blood to varying shear stress and exposure time to the shearing device fabricated with the design of the RIT Left Ventricular Assist Device (LVAD).

1.1 **Background**

1.1.1 Blood

The blood in our body contributes to 7-8% of our body weight. In addition, it plays a vital role in our immune system and in maintaining a relatively constant body temperature[5]. Of the 4000 different kinds of elements found in human blood, the four of the most important are the red blood cells, white blood cells, platelets, and plasma. The blood density in an average human is a constant value of 1050 kg/m^3. Since the viscosity of blood is shear thinning, at higher shear rates, it reaches a constant value[6-8].

1.1.1.1 Erythrocytes (Red Cells)

Red cells, or erythrocytes, are relatively large microscopic cells (7-10 μm), which make up 40% to 50% of the total blood volume[9]. The RBC's are produced continuously in the bone marrow from stem cells at the rate of 3 million cells per second. The process of production of the red blood cells is known as erythropoietin and these cells are biconcave discs with a diameter of 7 –10μm as shown in Figure 1.

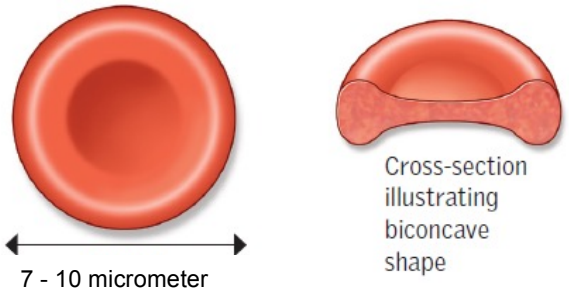

Figure 1: Red blood cell[23]

The life span of erythrocytes is 120 days and when they wear out, the main constituent, hemoglobin, explodes into compounds of iron, pigment, and amino acids that are eventually ingested by macrophages.

1.1.1.2 Leukocytes (White Cells)

White cells, or leukocytes, exist in variable numbers and types, but make up a very small part of the blood volume, normally only about 1% in healthy people. They occur elsewhere in the body as well, most notably in the spleen, liver, and lymph glands[5].

1.1.1.3 Thrombocytes (Platelets)

Platelets, or thrombocytes, are cell fragments without nuclei that work with blood clotting elements at the site of wounds. Platelets are smaller (2-3μm) than red blood cells and are also produced from stem cells in the bone marrow. They help in clotting by adhering to the walls of blood vessels, thereby plugging the rupture in the vascular wall. They also can release coagulating chemicals that cause clots to form in the blood that can plug up narrowed blood vessels. Platelets are not equally effective in clotting blood throughout an entire day. The body's circadian rhythm system (its internal biological clock) causes the peak of platelet activation in the morning. This is one of the main reasons that strokes and heart attacks are more common in the morning[5]. Recent research has shown that platelets also help

fight infections by releasing proteins that kill invading bacteria and other microorganisms. In addition, platelets stimulate the immune system.

1.1.1.4 Plasma

Plasma is the relatively clear, yellow tinted aqueous (92%) solution of sugar, fat, protein and salt that carries the red cells, white cells, and platelets. Normally, 55% of our blood's volume is made up of plasma. As the heart pumps blood to cells throughout the body, plasma brings nourishment to them and removes the waste products of metabolism. Plasma also contains blood clotting factors, sugars, lipids, vitamins, minerals, hormones, enzymes, antibodies, and other proteins[9].

1.1.2 Blood damage

Blood damage by fluid forces primarily depends on the magnitude and duration of shear stress. The two types of damage that blood handling device designers are concerned with are hemolysis and thrombosis[7].

1.1.2.1 Hemolysis

Hemolysis is the destruction of red blood cells, caused by disruption of the cell membrane and resulting in the release of hemoglobin (shown in Figure 2). Hemolysis is seen in some types of anemia, which can be either inherited or acquired, as by exposure to toxins or by the presence of antibodies that attack red blood cells[11]. During hemolysis the cells burst thereby releasing their contents such as hemoglobin into the surrounding plasma. Hemolysis induced by mechanical shear stress is a topic of interest in this thesis.

Figure 2: Process of Hemolysis in a Red blood Cell[20]

1.1.2.2 Thrombosis

Thrombosis is the formation of a blood clot in the vessels due to an obstruction in the flow (Figure 3). The most common place these blood clots occur are in the veins where they can cause severe injury[12]. Although the initiation of clotting can be triggered by high shear stress, it is not the subject of this thesis. This damage usually occurs if the mechanical devices such as the shearing device and LVAD pumps are not cleaned properly before blood is passed through them.

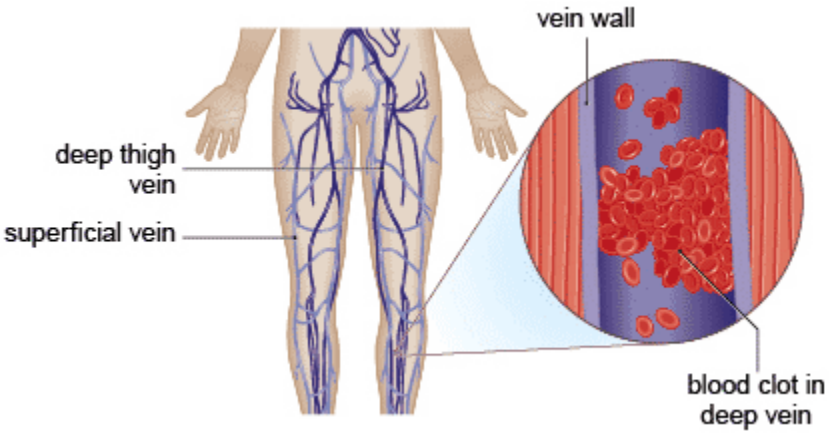

Figure 3: Deep vein Thrombosis[22]

1.1.3 Blood shearing devices

Blood pumps are mechanical devices that use mechanical pressure to move blood. Blood shear devices are used to assist the development and application of blood contacting pumps to study the relationship

between blood damage and flow dependent parameters[4]. One of the most recent studies of shearing devices was done by Zhang et al. Zhang et al. studied two devices, namely the Hemolyzer-H and Hemolyzer- L. The Hemolyzer- H was derived from the Adult Jarvik 2000 (shown in Figure 4(a)) and the latter was adapted from the CentriMag Blood Pump (shown in Figure 4(b)). The Hemolyzer-H (Figure 4(c)) had a gap between the inner rotor and the outer housing of 100 μ m. The rotational speed of the rotor was varied by the motor controller with a minimum increment of 10rpm.The Hemolyzer- L (Figure 4(d)) had a gap of 150 μ mbetween the housing and the rotor. The Hemolyzer- H had a mirror like surface finish (arithmetic mean roughness of a surface, Ra = 0.1 μ m) and the Hemolyzer- L had N5 (Ra = 0.4 μ m) on the wetted regions.

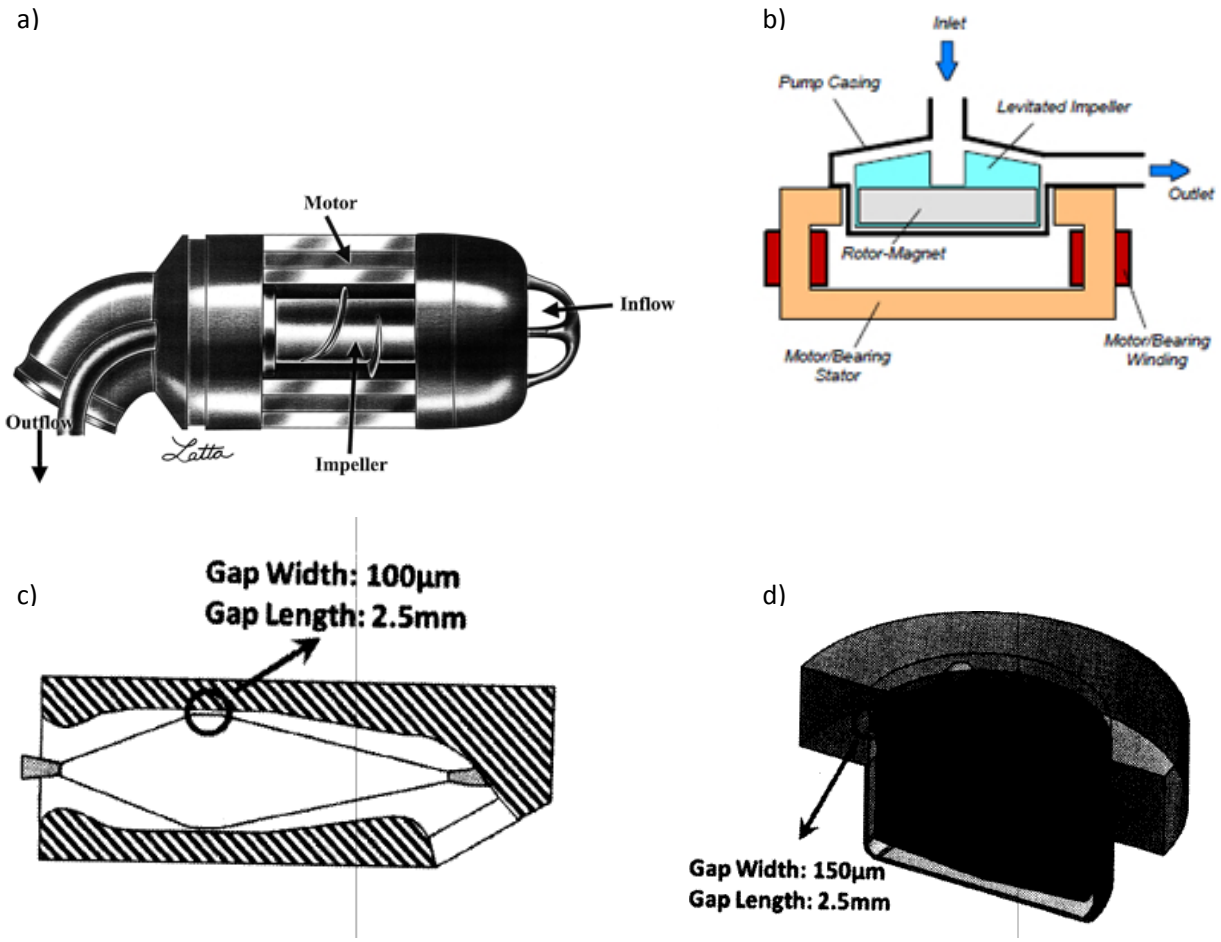

Figure 4: a) Jarvik 2000 blood pump, b) CentriMag blood pump, c) Schematic of Hemolyzer- H, d) Schematic of Hemolyzer- L[4]

The shear stress produced by the Hemolyzer- H ranged from 117 and 338 Pa and for the Hemolyzer- L, it ranged from 21 Pa to 212 Pa for blood with viscosity of 0.0036 Pa.sec. In Zhang's research, the main goal was determination of flow induced hemolysis by varying shear stress and exposure time (shown in Figure 5). The results acquired were compared with the study done by Paul et al.[1].

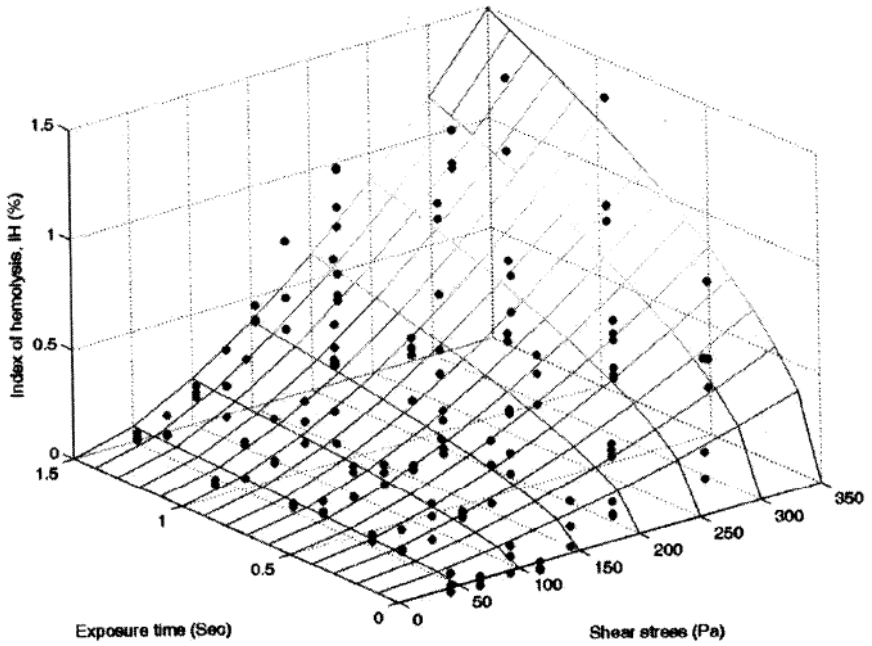

Figure 5: Relation between Hemolysis Index, shear stress and Exposure time obtained by Zhang's study[4]

In the device used for the Paul et al (Figure 6), RBC damage was not measurable below the shear stress of 425 Pa and exposure time shorter than 620ms, whereas for the same experimental domain, Zhang and his team determined a gradual increase in the hemolysis level. In this thesis, bovine blood will be used in the fabricated device to determine the damage induced in terms of shear stress and exposure time.

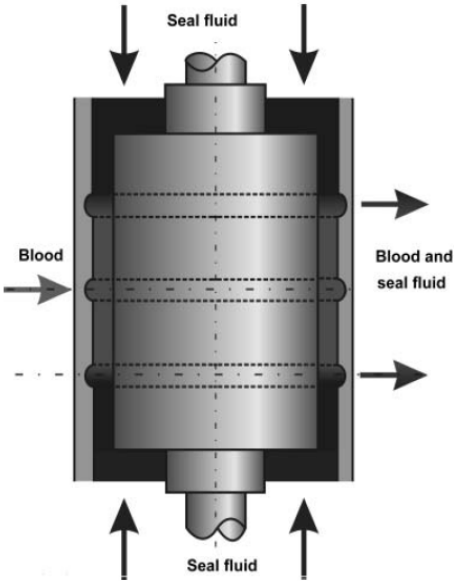

Figure 6: Schematic drawing of the shearing device used in the Paul et al. study[1]

1.1.4 Measurement of Free Hemoglobin and Index of Hemolysis

One of the most commonly known and trusted ways of physically determining the damage in the blood is by plasma hemoglobin measurement[16]. Malinauskas showed that hemolysis damage caused by medical devices could be determined. First, the samples were filtered and then underwent two levels of centrifugation in order to separate the plasma from the red blood cells. The first level of centrifuge was done for 15 minutes at 3500 RPM, thus isolating the plasma which was mixed with free hemoglobin (shown in Figure 7).

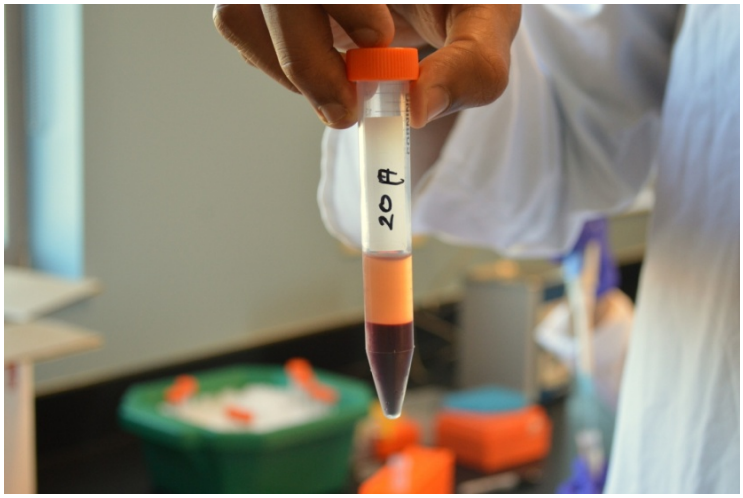

Figure 7: Centrifuged sample of damaged bovine blood

The second level of centrifuging was done for 15 minutes at 4200 RPM, which removes remaining red blood cells. This plasma was then displaced into cuvettes using micropipettes for further analysis. The color of the plasma darkens (Figure 8) as the degree of damage to the red blood cells increases.

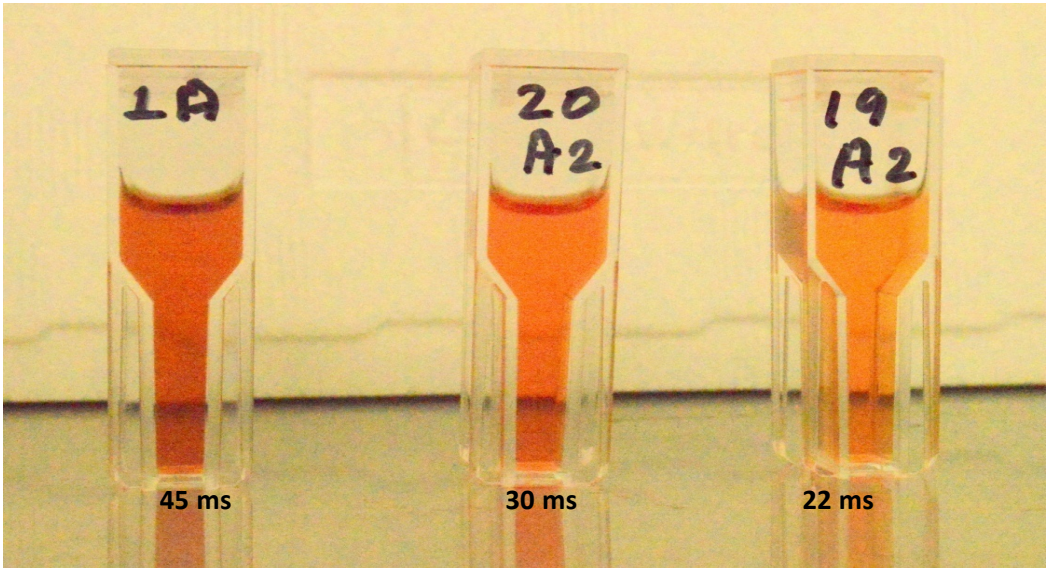

Figure 8: Plasma color darkening from right to left as the degree of damage increases

There are two techniques of classifying the plasma hemoglobin: an added chemical technique and a direct optical technique. The *added chemical technique* uses a reagent with hemoglobin that forms

colored reactions. The *direct optical technique* uses a spectrophotometer and is the preferred technique. The most common direct optical techniques are the Cripps, Kahn, Porter and Shinowara techniques of which the Cripps is the method used at RIT.

1.1.4.1 Cripps Method:

The Cripps method is used to determine the quantity of free hemoglobin in undiluted plasma. This method is based on the fact that free hemoglobin (fHb) has a unique absorbance spectrum so that the concentration can be quantitatively measured by comparing the absorbance values at three prescribed wavelengths. The advantage of using this technique is that the absorbance at A_1(576.5nm), which is the peak absorbance of the oxyhemoglobin, is corrected by using the absorbance on both sides of the peak A_2 (560nm) and A_3 (593nm)[17] (shown in Figure 9). Finally the free hemoglobin in plasma is determined by inputting the three absorbance values in Equation 2.

$$fHb = 177.68\ (A_1 - \frac{A_2 + A_3}{2}) \quad \textbf{(2)}$$

where fHb is free hemoglobin in mg/dL, A - Absorbance, A_1- Absorbance at wavelength of 576.5nm, A_2- Absorbance at wavelength of 560nm and A_3- Absorbance at wavelength of 592nm.

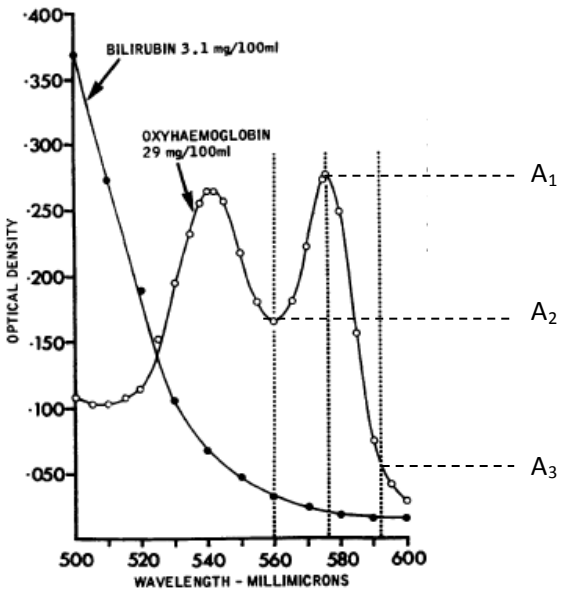

Figure 9: Graph that shows the Absorbance for wavelength of oxyhaemoglobin[17]

The Index of hemolysis (shown in Equation 3) is defined as the ratio amount of free hemoglobin in plasma normalized by the total amount of hemoglobin pumped through the device[24].

$$\text{I.H}\ (\%) = \frac{\text{fHb}}{\text{tHb}} * 100 \quad \textbf{(3)}$$

where I.H is the Index of Hemolysis (in %), fHb is free hemoglobin (in mg/dL) and tHb is total hemoglobin in blood. Bovine blood total hemoglobin ranges between 9500 mg/dL to 13500 mg/dL[25].

1.1.5 Maglev shearing device

Myagmar[19] designed the Maglev shearing device using CFD and began design modifications to create a shearing device (Figure 10) using the magnetic suspension from the RIT LVAD. Her work included design iterations of the rotor in order to achieve the desired range of shear stress and exposure time. For first order approximations, it is assumed that the Maglev shearing device has a Couette flow condition which creates a constant shear stress and CFD results prove this to be true. Her work shows that the

region 1 (gap region) provides a uniform shear stress throughout the region and, in region 2, the impact of shear stress is negligible (shear stress in inversely proportional to the gap).

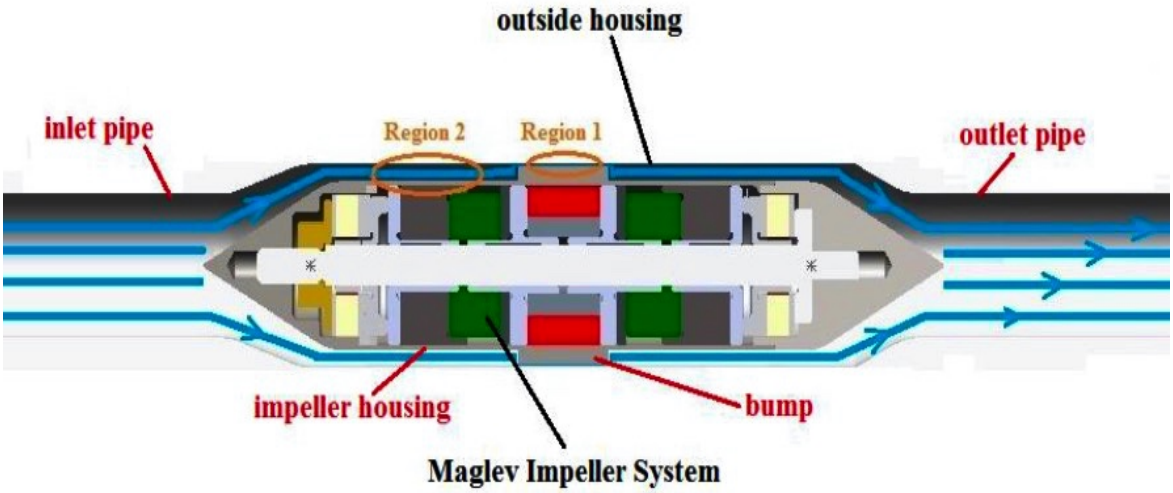

Figure 10: Maglev shearing device cross sectional view[19]

1.1.6 Taylor Vortex

The Taylor Couette flow (shown in Figure 11) arises from the shear flow of a viscous fluid in the gap between rotating cylinders and a concentric, fixed outer cylinder. Taylor offered a non-dimensional Taylor number, Ta, in order to determine the critical relative rate of rotation between the cylinders[15].Taylor vortices are formed when the Taylor number exceeds the critical Taylor number.

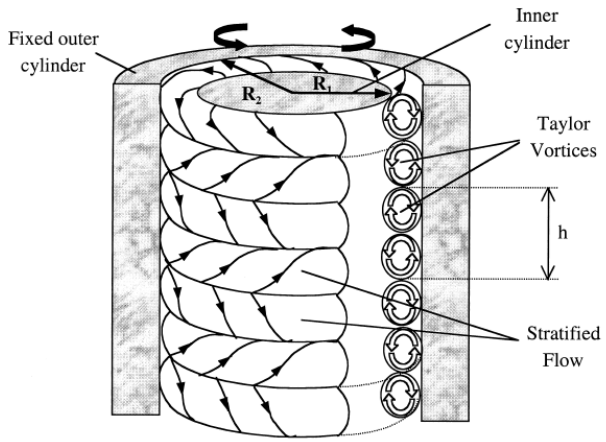

Figure 11: Taylor Couette flow and the formation of Taylor vortices[15]

1.1.7 Hemolysis Power Law models

The empirical power law model (Equation 1) is formulated on the assumption that there are only two factors in the determination of hemolysis. These power law models consist of correlation between observed damage (D) and both shear stress (τ) and exposure time (Δt).The two most commonly used power models that relate damage to shear stress and exposure time are shown in equations 4 and 5.

The Giersiepen Power law model as Equation 4 and Heuser's power law model as Equation 5 was derived by regression analysis of their individual experimental data.

$$D = 3.62 * 10^{-7} \tau^{2.416} \Delta t^{0.785} \quad \textbf{(4)}$$

$$D = 1.8 * 10^{-6} \tau^{1.991} \Delta t^{0.765} \quad \textbf{(5)}$$

1.2 Motivation

Implantable ventricular assist devices are regarded as dependable and promising for patients with severe heart failures[8]. These pumping devices support the affected heart in its regular pumping process[13]. Some of the major pumps that are used for this purpose are rotary pumps and centrifugal pumps. All rotary pumps approved for clinical use have some type of mechanical bearings and considerable design effort has been put into designing these bearings to reduce mechanical wear and to reduce hemolysis in pumps with mechanical bearings[14]. Nonetheless, there are recently published reports of large trials of 2nd generation devices (rotary pumps using mechanical bearings) that show improved survival and decreased thromboembolic complications as compared with pulsatile devices. The LVAD blood pump

(Figure 12) created at RIT is an axial flow pump that has a simple, unobstructed single blood flow path and novel hybrid magnetic bearings that can overcome the strong axial forces on the rotor without compromising the idealized flow path[14]. Due to the inherent nature of blood contacting devices, the various components of blood are subjected to shear stresses caused by the device. The accurate analysis and prediction of blood damage during the design phase of the device has been difficult to achieve. Hence the analysis of this preliminary design was numerical and the device was not constructed.

Figure 12 : Blood Pump at RIT

1.3 **Objectives**

a. To fabricate a robust magnetically suspended system that can expose blood cells to known and controllable shear.

b. To use this device to damage the blood cells at varying shear stresses for known amount of exposure time.

2 METHOD

The goal of this thesis was to fabricate a device which damages the blood at varying shear stresses for known amounts of exposure time. The work done to achieve this goal is discussed in section 2.1 and the damaging of blood by varying shear stress and exposure time is discussed in section 2.2.

2.1 Experimental Apparatus

This section discusses the Maglev shearing device parts and flow parameters.

2.1.1 Maglev Components and Parts

The Maglev shearing device in this thesis is used to determine the blood damage with varying exposure time and shear stress. The base structure consists of the pump like assembly with the five major parts kept together in sequence with appropriate distances from each other. This design refers back to the initial design of the LVAD pump. The major parts of the shearing device, including the active components, are shown using the cross sectional view of the shearing device (Figure 13).

1. Magnetic system from the LVAD pump
2. Outer housing
3. Rotor rear
4. Rotor front
5. Bump
6. Outlet pipe
7. Inlet Pipe

Active components

A. Front Hall Effect Sensor Arrays (HESA)

B. Front Active Magnetic Bearings (AMB)

C. Motor

D. Rear Active Magnetic Bearing (AMB)

E. Rear Hall Effect Sensor Array (HESA)

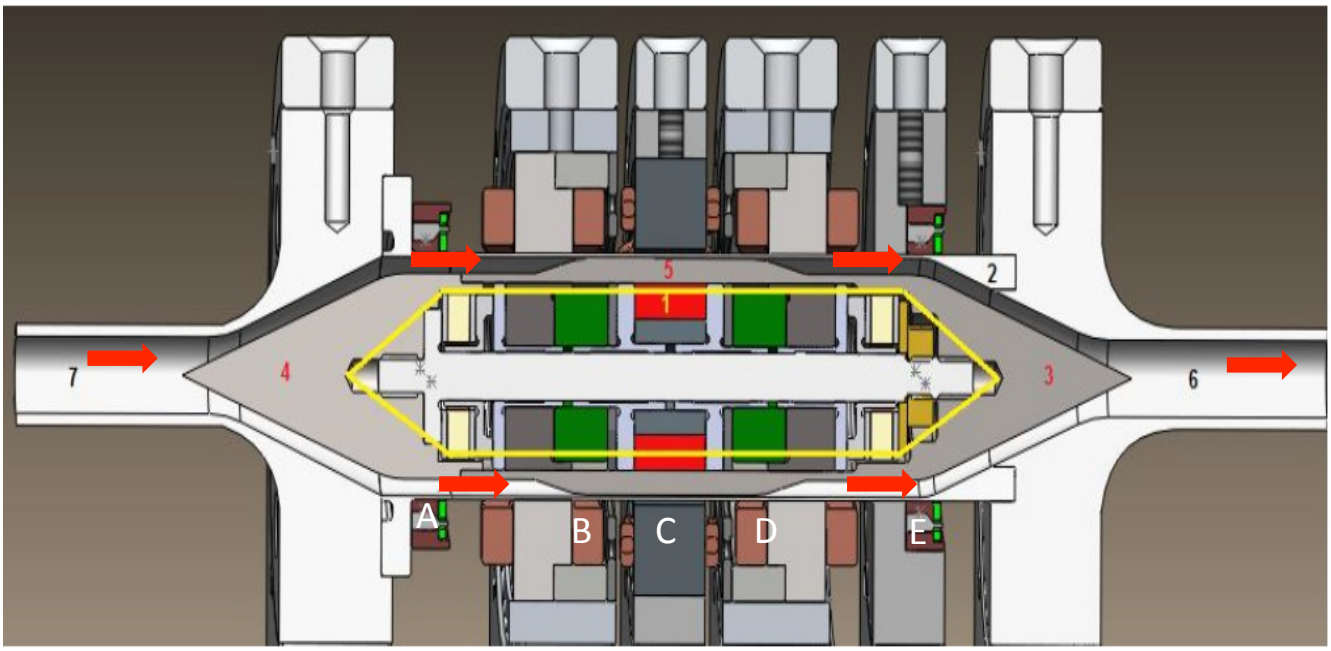

Figure 13 : Cross sectional view of the Maglev shearing device[19]

2.1.1.1 HESA

The HESA is a set of four sensors which are placed around the ends of the housing cylinder. Hall Effect Sensors are sensors that vary the voltage when the magnetic field changes. The sensors are used to detect the permanent magnet filled rotor's movements in any direction within the housing cylinder. These HESAs (shown in Figure 14) are custom made to solve our purpose of positioning around the housing cylinder.

Two HESAs are used in this device, namely the front and the rear HESA. Each array consists of four sensors with 6 wires – 4 from the sensors, 1 to the ground and 1 from the power supply. The sensors are named as H_{FXP} (HESA Front X positive), H_{FYP} (HESA Front Y positive), H_{FXN} (HESA Front X negative), H_{FYN} (HESA Front Y negative), H_{RXP} (HESA Rear X positive), H_{RYP} (HESA Rear Y positive), H_{RXN} (HESA Rear X negative), and H_{RYN} (HESA Rear Y negative).

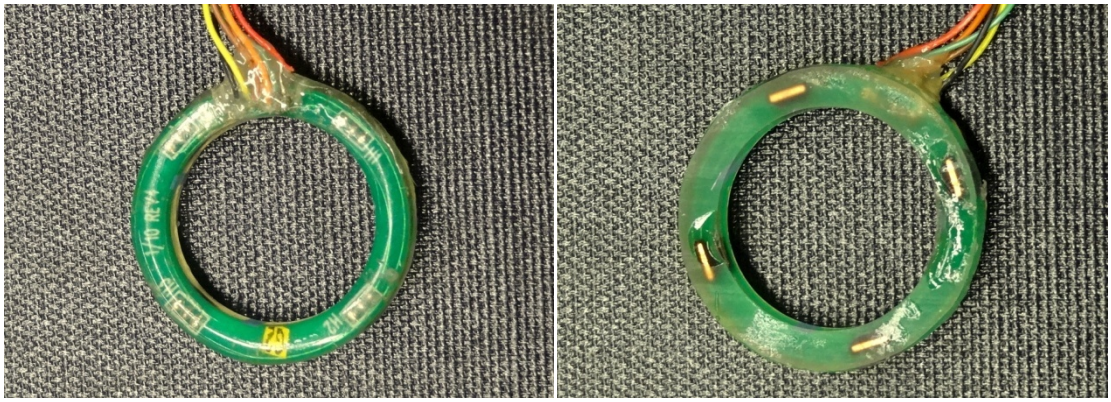

Figure 14 : Custom made HESA used in the shearing device

2.1.1.2 AMB

The AMB is a set of coil windings around the housing cylinder for the front and the rear of the shearing device. There is AMB (Figure 15) in the front and the rear of the device namely the Front AMB and the Rear AMB, respectively. The AMB uses electromagnetic force to levitate, maintain the position, and permit relative motion of the rotor, which is filled with permanent magnets. The front AMBs consists of four windings named FXP (Front X positive), FYP (Front Y positive), FXN (Front X negative), FYN (Front Y negative) and consequently, the rear windings are named as RXP (Rear X positive), RYP (Rear Y positive), RXN (Rear X negative), RYN (Rear Y negative).

Figure 15 : Rear AMB on the shearing device

2.1.1.3 Motor

A three phase brushless motor is used in this device. The stator holds six coils and all of them are connected in the delta configurations shown in Figure 16. The motor houses a four-phase magnet and the rotating magnetic field is created by the sequential excitation of the pole parts by a DC pulse[18].

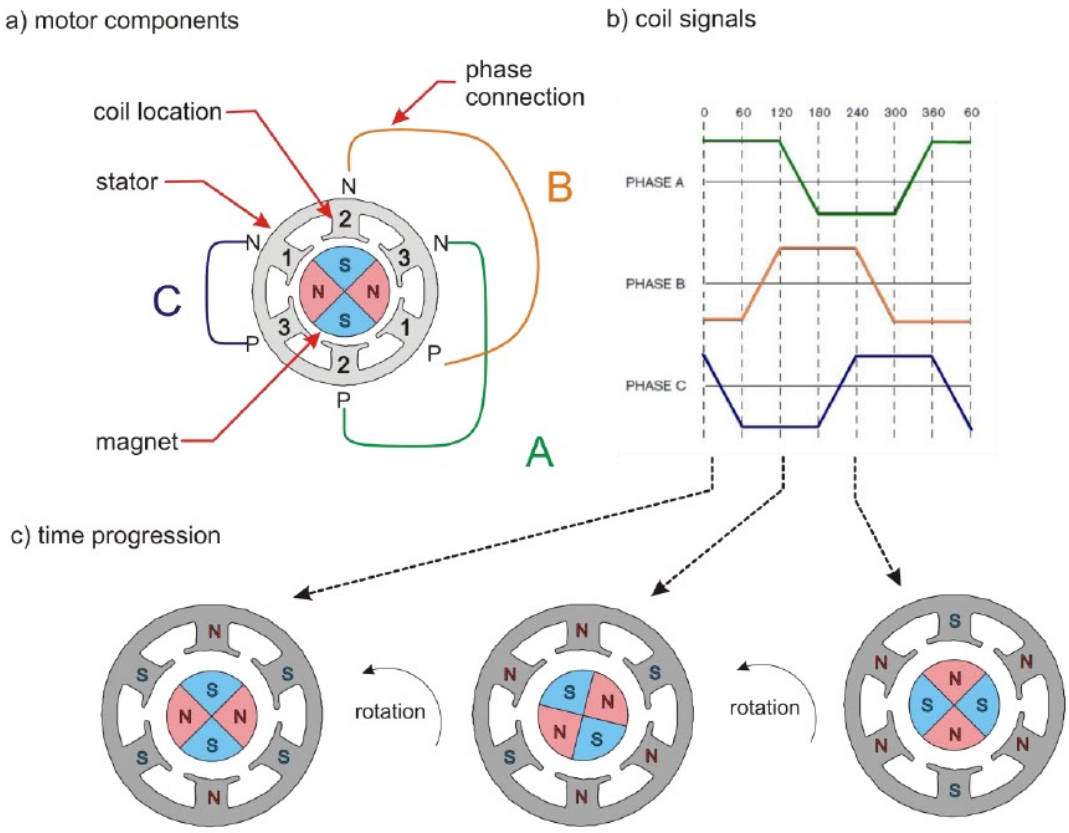

Figure 16 : Three Phase brushless motor[18]

The three active components come around a housing cylinder, where the rotor is made to levitate and spin. The inducer and the diffuser, which were specifically manufactured to the flow of our design, are connected at the front and the rear of the shearing device respectively.

The wiring from the all the AMB's, HESA's and the motor phase are screwed to the terminal junction box (Figure 17), which is then routed to the target system. The magnetically levitated system is completely controlled by the target system and executed within Microsoft Windows operating system.

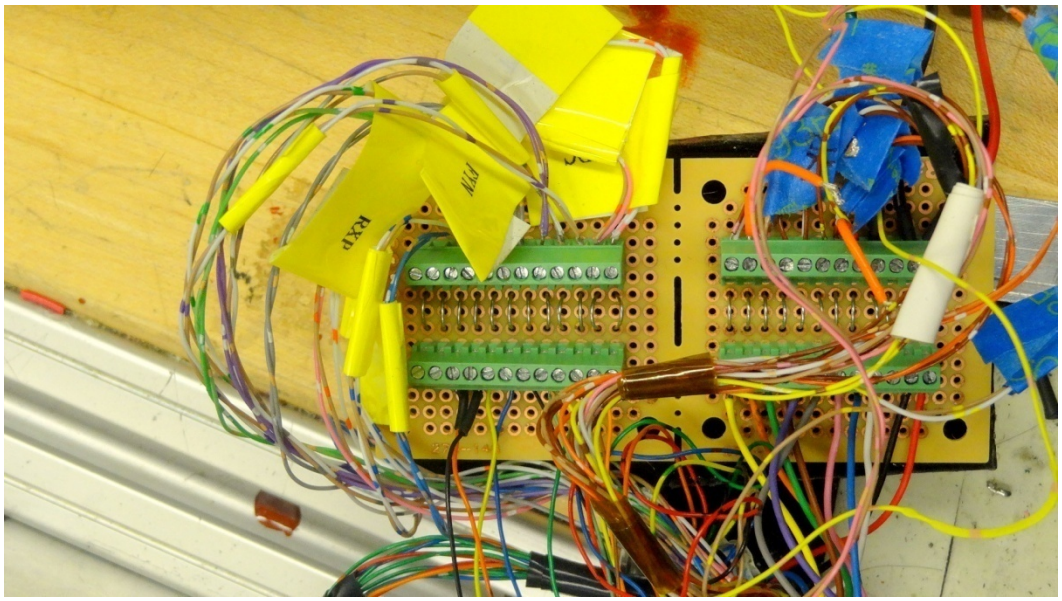

Figure 17 : Bread board connection for wires from and to the shearing device

2.1.1.4 Outer Device Case

The shearing device is covered with a case made by 80-20 1 inch structural beams and acrylic panels (shown in Figure 18). The case protects the shearing device from unnecessary human contact, fluid spills on the device and other factors.

Figure 18 : Protective outer case for the shearing device

2.1.2 Flow Path Design

The flow path is constructed in such a way that, the blood is pumped at a flow rate Q into the device and sampled at the end of the device as shown in Figure 19. The shearing device uses a bladeless rotor, so it cannot by itself pump the blood. The 2nd major objective of this thesis is to determine the damage to the blood due to varying exposure time and known amount of shear stresses uniformly across the gap. In order to implement this practically, the relationship between shear stress and exposure time with individual criteria needs to be determined separately.

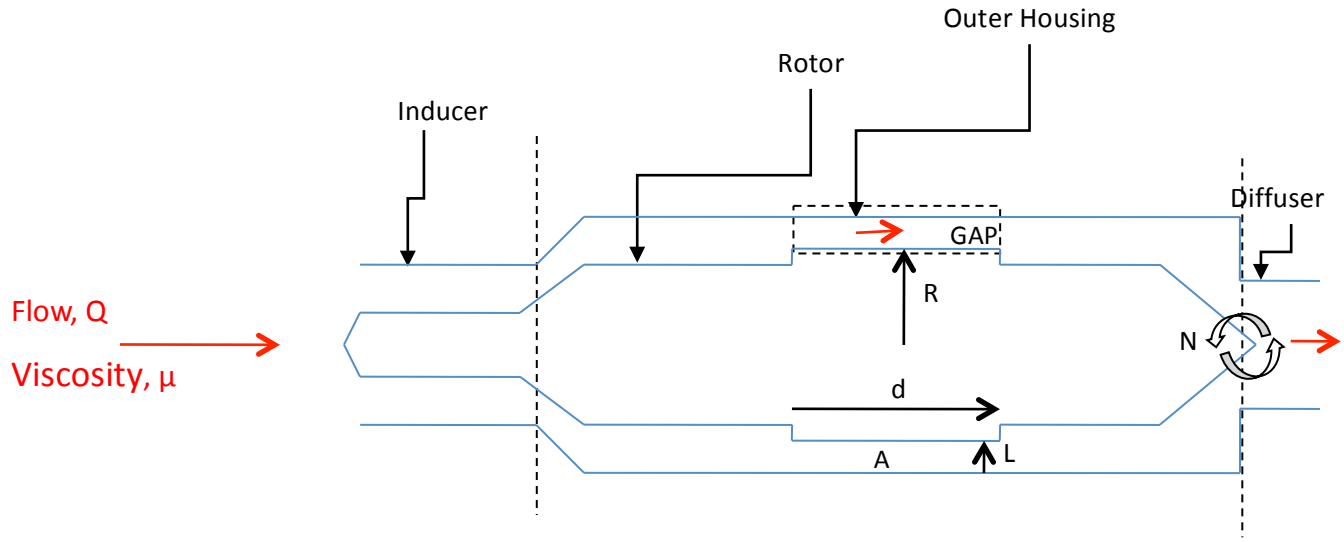

Figure 19 : Flow path of the shearing device

2.1.2.1 Exposure time (Relationship between Exposure time and flow rate)

The flow rate depends on the area and the velocity of the fluid entering the cross section (shown in Equation 6).

$$Q = \frac{Ad}{\Delta t} \quad (6)$$

where A is the Area of the cross section, Q is the Flow rate, d is the Shear gap Length (27 mm), and Δt is the Exposure time.

The exposure time is inversely proportional to the flow rate ($Q \propto \frac{1}{t}$). Hence exposure time is varied by varying the flow rate of the fluid entering the shearing device.

In order to determine uniform exposure time through the gap, the assumption is made that the velocity is uniform throughout the flow in the axial direction as shown in

r

Figure 20.

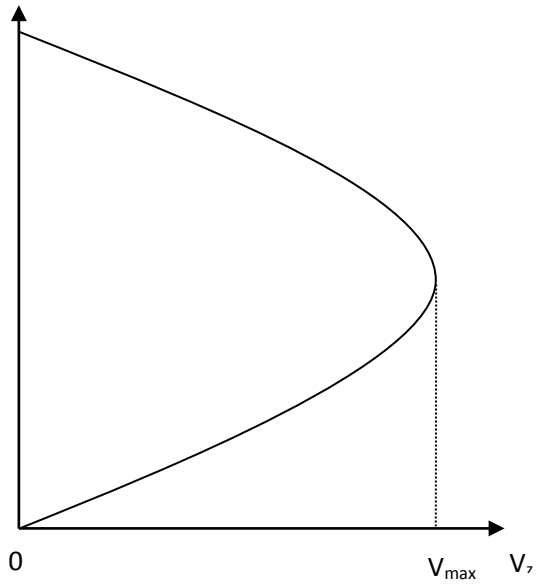

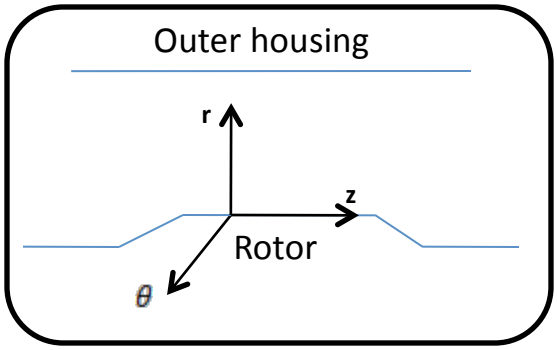

Figure 20 : Velocity profile of the axial direction in the gap region

2.1.2.2 Shear stress (Relationship between Shear Stress and rotor speed)

From prior CFD calculation, it is confirmed that the shear damage is maximum at the gap. Using the circumferential direction of the flow in the device, shear stress can be related to the rotor spinning (Equation 7a and 7b) inside the housing cylinder as shown in Figure 21.

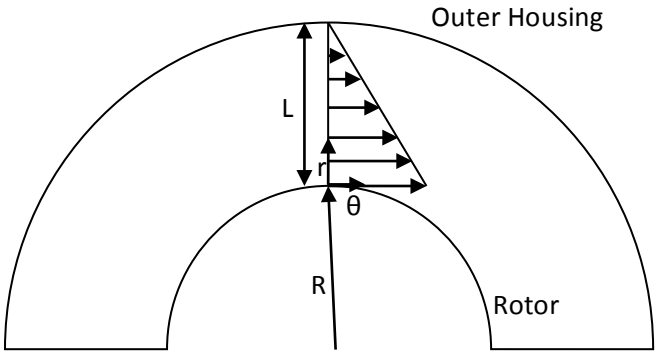

Figure 21 : Cross sectional view of the gap region in the circumferential direction for shear stress to rotor speed derivation

$$\tau = \frac{\mu \omega R}{L} \quad \textbf{(7a)}$$

$$\tau = \frac{2\pi \mu R N}{60L} \; [\omega \text{ (in rad/sec)} = 2\pi N/60] \quad \textbf{(7b)}$$

where τ is the shear stress, μ is the viscosity of blood (4.5cP), R is the radius of the rotor (9.55mm), L is the Gap height (0.23mm) and N is the rotor spinning speed (in RPM). The shear stress is directly proportional to the rotor speed ($\tau \propto N$), hence shear stress is increased and decreased by varying the spinning of the rotor inside the housing cylinder.

The assumption is made that the shear stress in the circumferential direction is much higher than the shear stress in the tangential direction. Thus the shear stress in the tangential direction (

Figure 22) is insignificant.

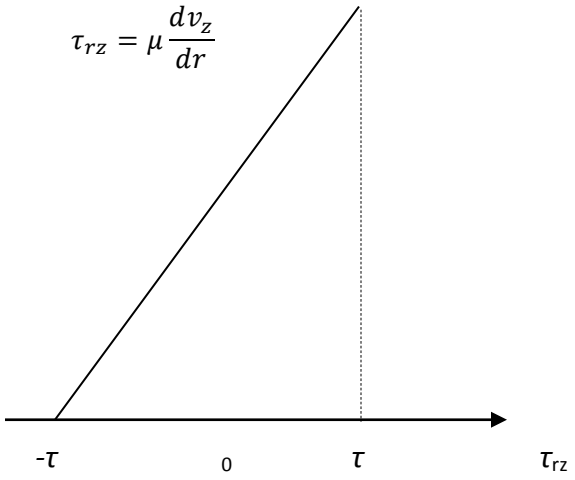

Figure 22 : Shear stress profile for the tangential direction

The shear stress profile of the circumferential direction, which is uniform through the gap region, is drawn from the velocity profile of the same direction (shown in Figure 23).

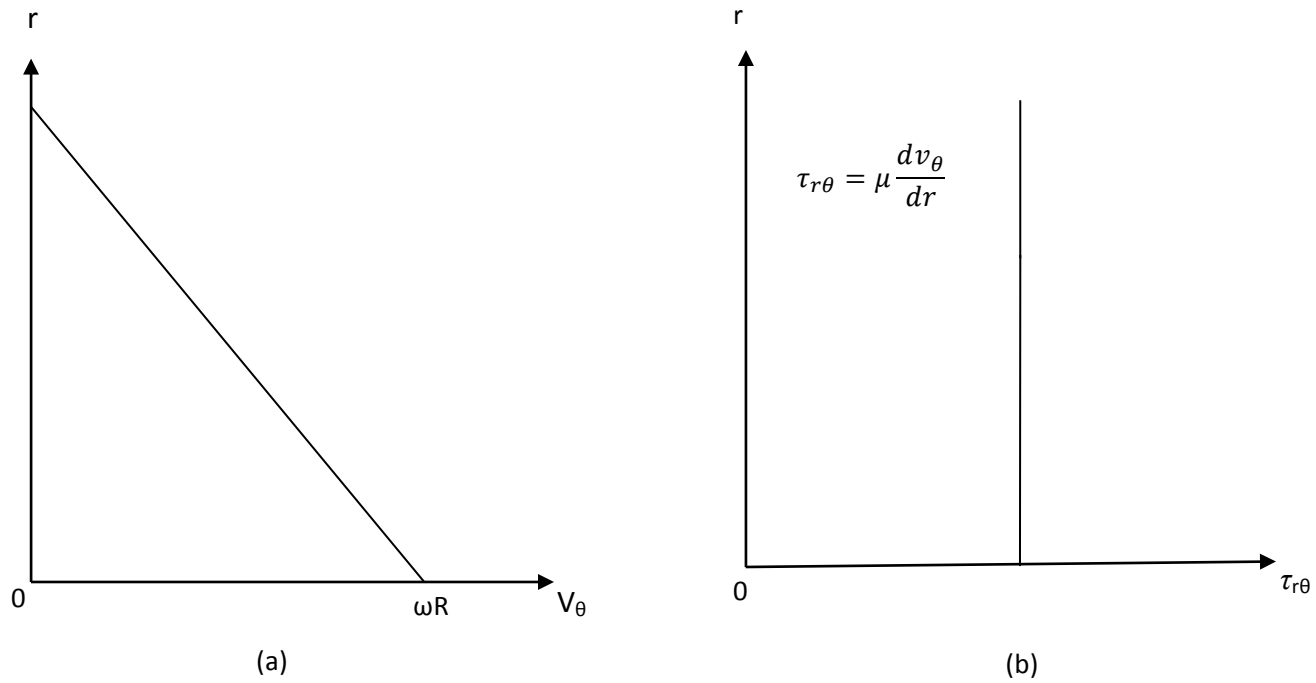

Figure 23: (a) Velocity profile and (b) shear stress profile of the circumferential direction of the shearing device

2.1.2.3 Rotor Speed determination

A dynamic signal analyzer was connected to one of the signals from either the front or the rear HESA. This signal was then read using FFT from a dynamic signal analyzer (Figure 24) to determine the frequency and in turn, the speed of the rotor.

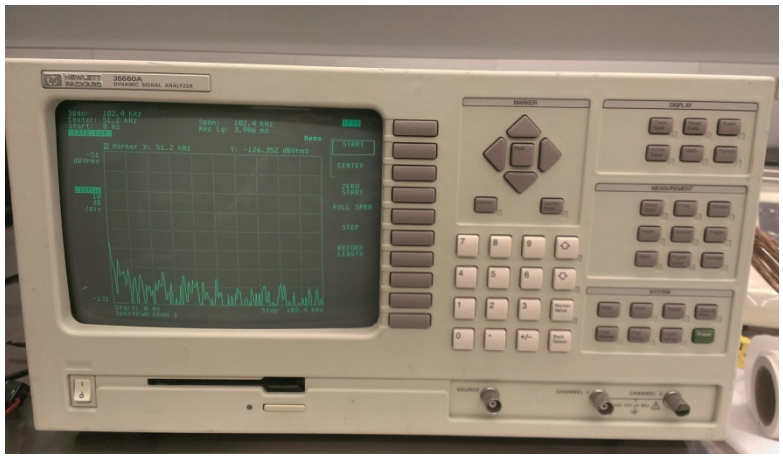

Figure 24: Photograph of the dynamic signal analyzer which was used to determine the speed of the rotor

2.2 **Blood Damage Measurement**

The shear stress is varied by altering the rotational speed of the rotor and the exposure time is varied by altering the volume flow rate of the syringe pump.

The dump time, T_D, (Equation 8) is defined as the time taken for the damaged blood from the gap region to reach the sampling region (3 way valve).

$$T_D = \frac{\text{Volume(from the shearing gap region to the sampling region)}}{\text{flow rate of the fluid}} \quad \textbf{(8)}$$

The experiment to determine the blood damage is set up exactly as shown in Figure 25. Thermocouples were inserted in order to determine the inlet and outlet temperature of blood. The speed of the rotor is determined from the frequency acquired from the digital analyzer, which is connected to the rear HESA signal.

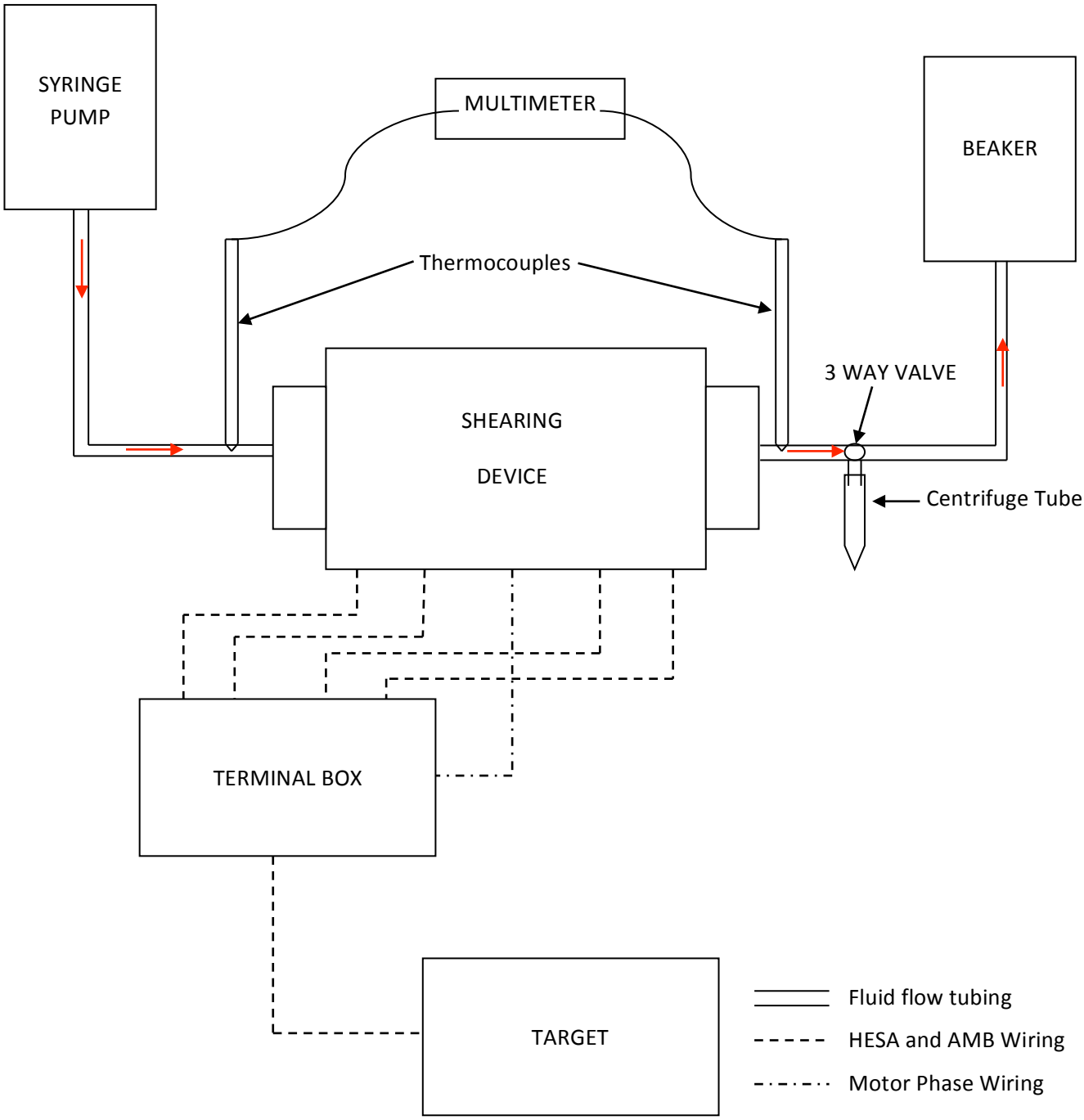

Figure 25: Blood damage measurement experimental set up

2.2.1 Sampling Procedure

The Sampling procedure is the process of sampling blood, which was damaged in the gap region (shown in Figure 246), in the centrifuge tubes for a particular shear stress and exposure time set up in the device.

1. Tubing and fittings are fitted at the appropriate location and all exits are sealed except for the sampling exit.
2. Start rotor levitation.
3. Pump blood through the shearing device using the syringe pump at a flow rate of 4ml/min.
4. Start taking time measurements using a stopwatch as soon as the required rotor speed and flow rate of blood are set.
5. Once the dump time is reached for a particular flow rate, the sampling of the blood is done by changing the flow direction on the 3-way valve to let the damaged blood be collected in a centrifuge tube.
6. Once the required amount of blood sample is collected, the flow direction on the 3-way valve is returned to original and the blood flow goes back to the beaker.
7. Steps 4 to 6 are repeated for different rotor speeds and flow rates.

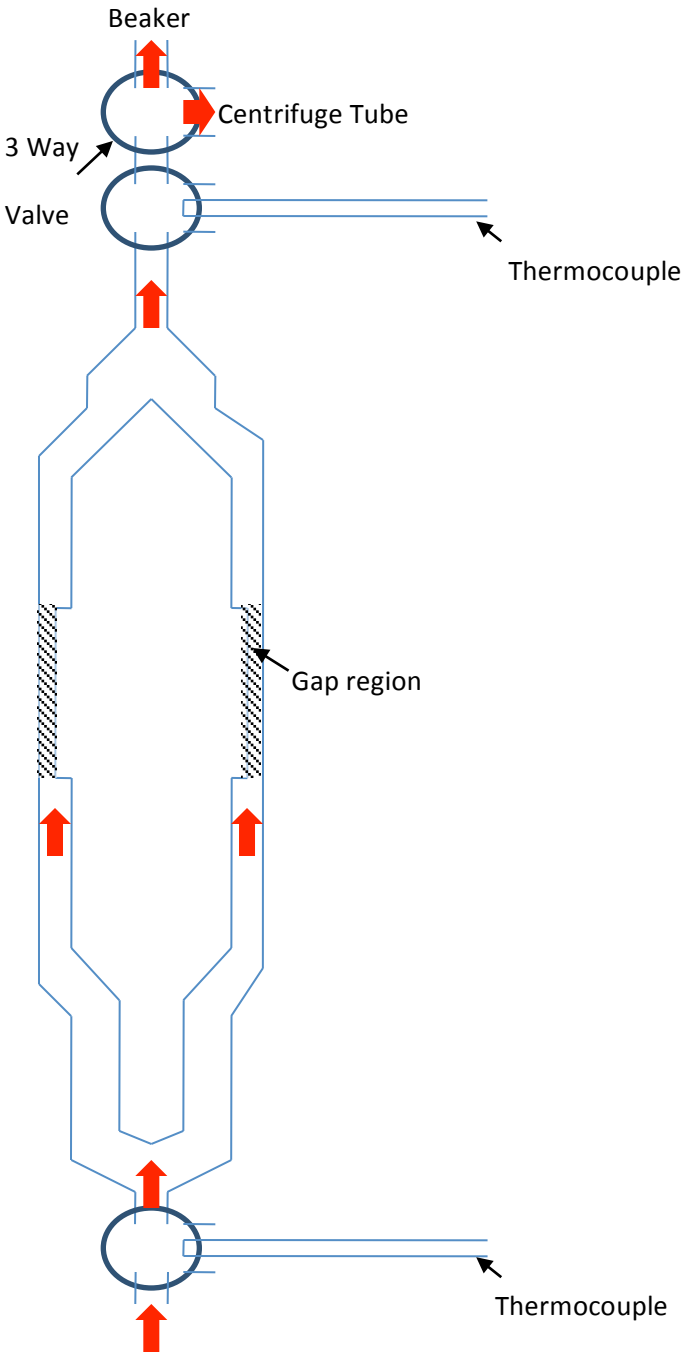

Figure 246: Flow of blood in the shearing device for sampling

The samples were centrifuged in centrifuge tubes, stored in cuvettes (Figure 257), and then analyzed using the Cripps method in order to determine the Index of Hemolysis (as explained in the section1.1.4). The results of Cripps method is fHb in units of mg/dL. This was converted to I.H (%) according to the

Equation 3 assuming a total hemoglobin of 12000 mg/dL (mean of the reported range of 9500 mg/dL to 13500 mg/dL). The total hemoglobin was not measured directly.

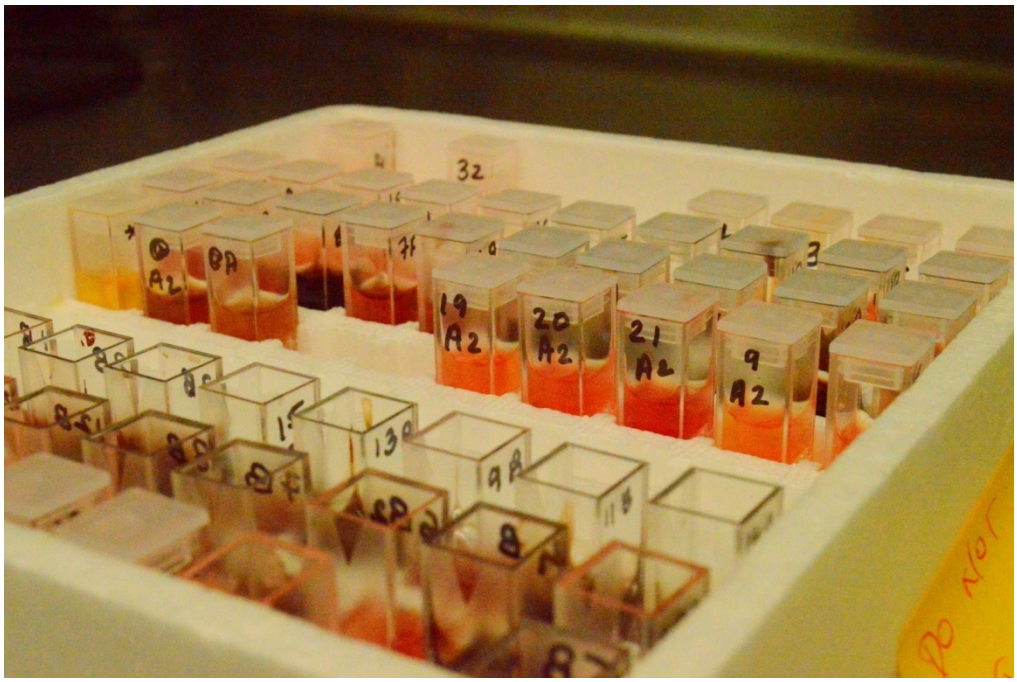

Figure 257: Plasma after two cycles of centrifuge stored in cuvettes

Before the actual blood damage measurement, the blood samples were passed to a centrifuge tube using the syringe pump, tubes, and tube fittings (the same tubes and tube fittings were used in the actual blood damage measurement as well) without passing through the device. After which centrifuge tube underwent the Cripps method and I.H was determined. The results showed that the samples (Figure 28) experienced negligible damage (low I.H (%) value) of 0.002%. This experiment was conducted 3 times and all results showed similar I.H value.

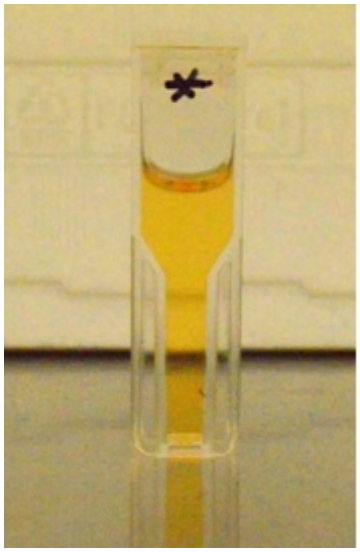

Figure 28: Plasma sample showing negligible blood damage when passed through the syringe pump and tubes alone

The blood used for all testing purposes was bovine blood and the Index of Hemolysis for varying shear stress and exposure time was determined in Trial #1.

2.2.2 Trial #1

The device was kept in a box with a fan running continuously in order to cool the device (shown in Figure29) and also in order to determine the temperature of the blood, thermocouples were added to the inlet and outlet of the shearing device. The shear stress was ranged from 0 Pa to 125 Pa and exposure time was ranged between 20ms to 70ms for this trial.

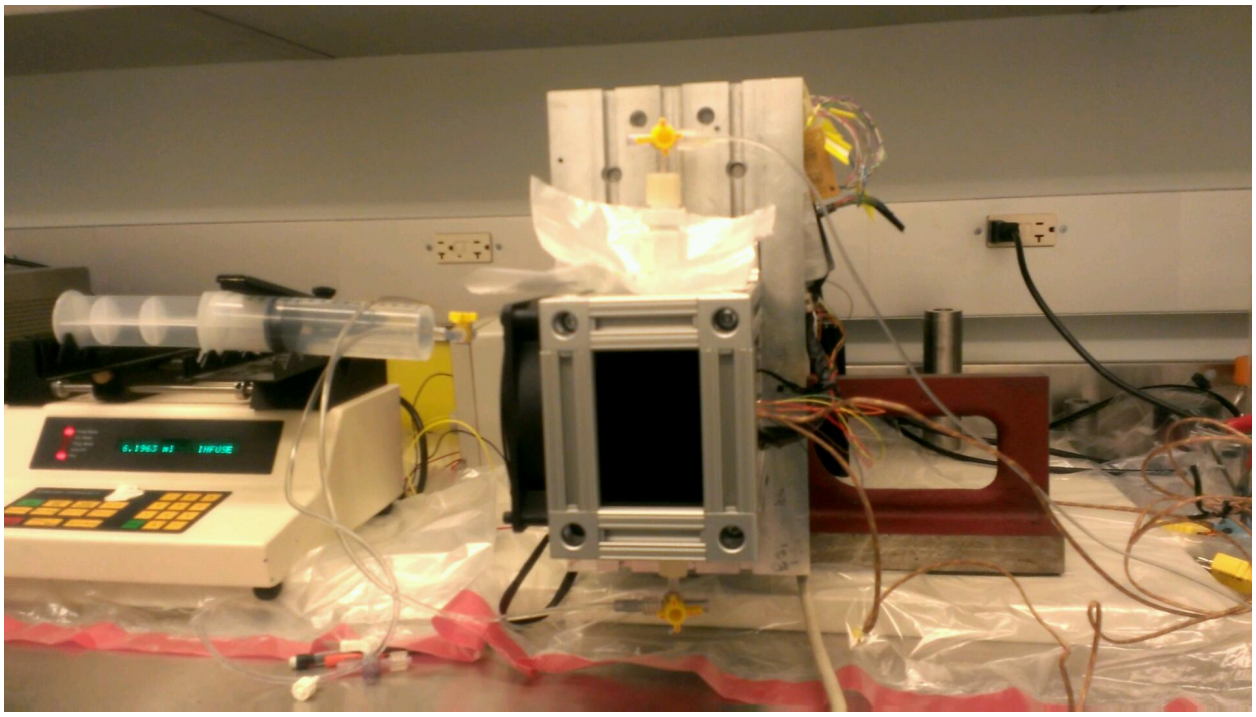

Figure 29: Set up of the blood shearing experiment Trial #1

The inlet and outlet temperature recorded during each sample taken was graphed with respect to the rotor speed (Figure 30).

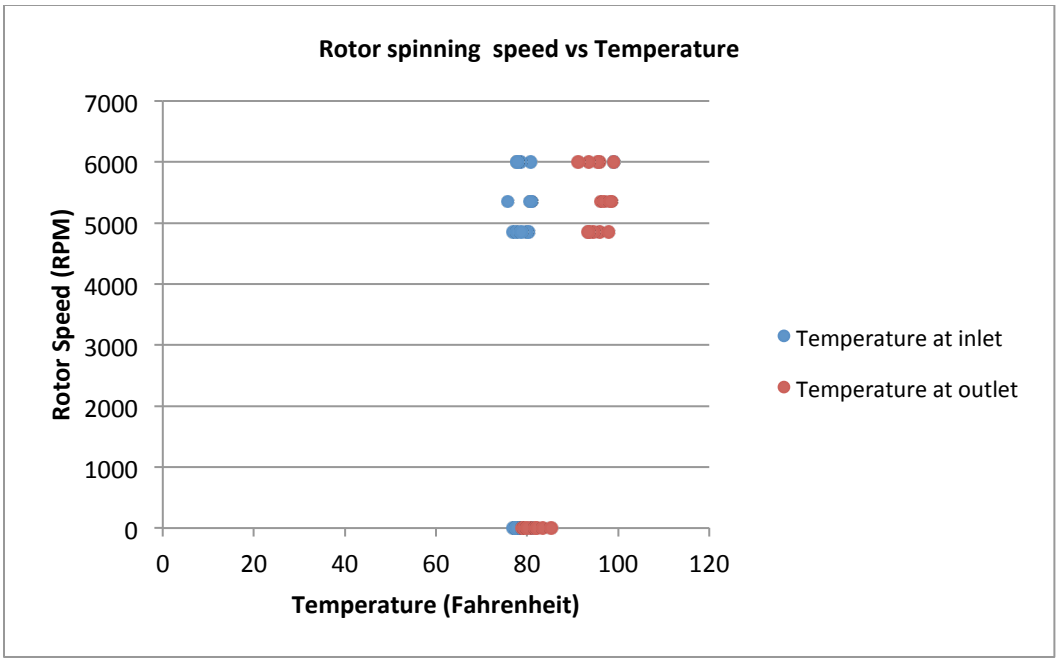

Figure 260: Rotor speed to the inlet and outlet temperature recorded for each sample

2.2.3 Trial #2

The setup of Trial #2 was exactly the same as Trial #1 (Figure29). There was a significant variation of temperature of the blood from the inlet to the outlet of the device during spinning (Figure 30). Hence this trial was conducted to determine the variation of damage due to change in temperature during levitation and not during spinning. Thus heat was physically induced to the system by changing the Proportional gains (P gains) of the Proportional-Integral-Derivative controller (PID controller) from the target system. By increasing the P gains more than usual, more current flows through the electromagnets and this unnecessary current is converted into heat. The heat is dissipated to the blood flowing through the device, thus raising the temperature of the blood.

The temperature of the blood is varied during levitation, by varying the gains, in order to produce similar temperatures that occurred during spinning in Trial #1. The temperature of the blood was varied from 80 ^{o}F to 100 ^{o}F for an exposure time range of 20ms to 45ms.

3 RESULT

The Index of Hemolysis (I.H) for different shear stress and exposure times are determined during the Trial #1and recorded in Table 1.

Table 1: Measured Index of Hemolysis (I.H) at varying levels of shear stress and exposure time during Trial #1

Sample #	Shear Stress	Exposure Time	fHb	I.H
	Pa	ms	(mg/dL)	(%)
1	0	67	2	0.015
2	0	45	2	0.015
3	0	30	3	0.022
4	0	22	2	0.015
5	124	67	64	0.533
6	124	45	47	0.385
7	124	30	40	0.333
8	124	22	18	0.148
9	124	22	27	0.222
10	113	67	54	0.452
11	113	45	29	0.244
12	113	30	36	0.304
13	113	22	26	0.215
14	100	22	25	0.207
15	100	67	53	0.444
16	100	45	36	0.296
17	100	30	26	0.215
18	100	22	28	0.237
19	0	67	5	0.044
20	0	45	5	0.044
21	0	30	5	0.044
22	0	22	18	0.148

A graph was plotted between I.H and exposure time for varying shear stress as shown in Figure 271. The I.H increases from 0.15 % to 0.55 % as the exposure time increases from 20ms to 70ms. The curves were drawn by the linear regression of experimental data of the I.H and exposure time for varying shear stress. The I.H was similar for the 100 Pa (slope = $0.007ms^{-1}$) and 113 Pa (slope = $0.0071ms^{-1}$) shear

stress for the range of 20ms to 70ms exposure time. The I.H of 124 Pa was slightly higher (slope = 0.0085ms^{-1}) than that of the 100 Pa and 113 Pa for the same range of exposure time. All the experiments in trial #1 were conducted in the time period of 48 hours. The 0 Pa (rotor levitation only) shear stress was noted before the start and the finish of the experiment for different exposure times. The I.H of the reading after 48 hours was recorded to be slightly higher (0.025 %) than that at the start of the experiment due to aging in blood.

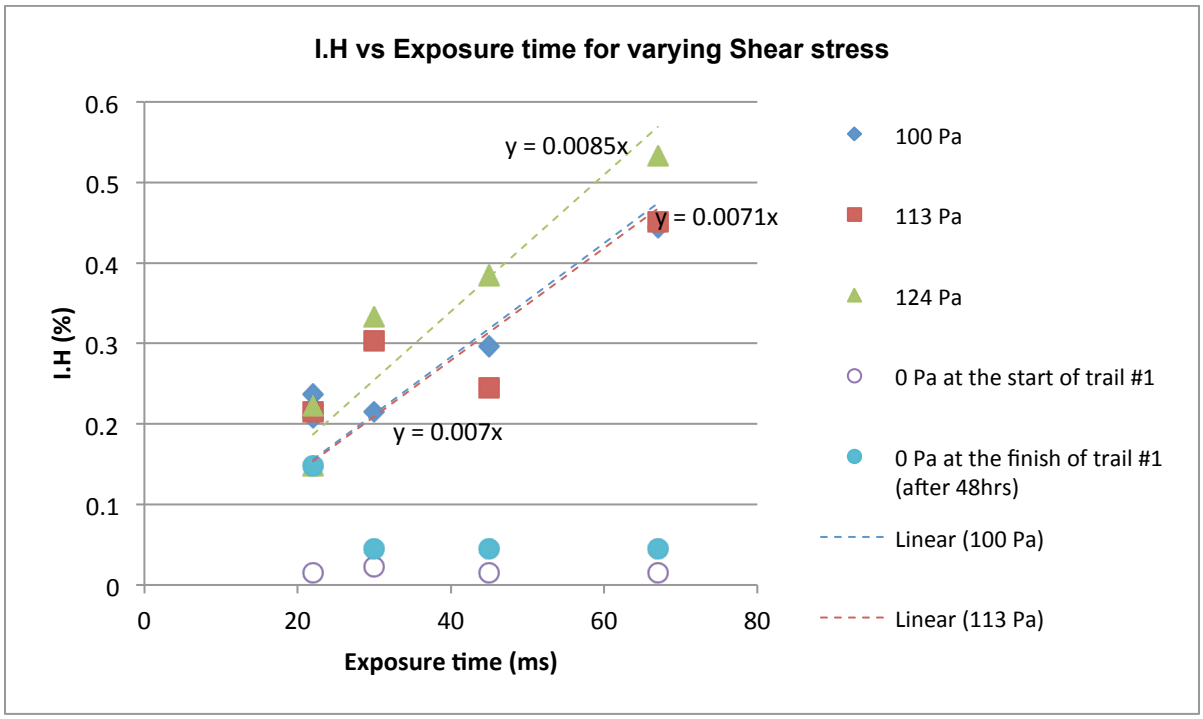

Figure 271: I.H vs Exposure time for varying Shear Stress

A graph was also plotted between I.H and shear stress for varying exposure time as shown in Figure 282. The I.H increases from 0 % to 0.55 % as the shear stress increases from 0 Pa to 125 Pa. The curves were drawn by the linear regression of experimental data of the I.H and shear stress for varying exposure time. The I.H was similar for the 30ms (slope = 0.0025ms^{-1}) and 45ms (slope = 0.0028ms^{-1}) exposure

time for the range of 0 Pa to 125 PA shear stress. The I.H of 67ms was slightly higher (slope = 0.0042ms^{-1}) than that of the 30ms and 45ms, and much higher than that of 22ms (slope =0.0018ms^{-1}) for the same range of shear stress.

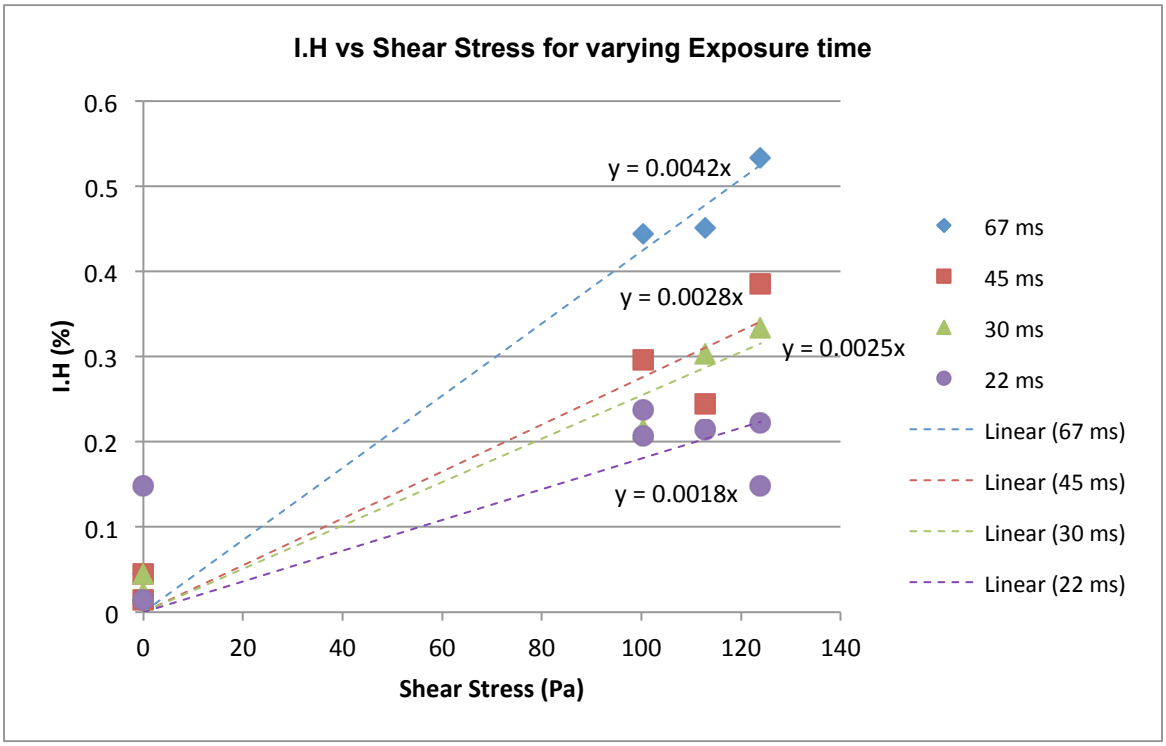

Figure 282: I.H vs Shear stress for varying Exposure time

In order to determine the damage due to temperature alone, I.H for different exposure times and temperature are determined at 0 Pa shear stress during Trial #2 and recorded in Table 2.

Table 2: Measured Index of Hemolysis (I.H) at varying levels of temperature and exposure time during Trial #2

Sample #	Shear Stress	Exposure Time	Temp	fHb	IH
	Pa	ms	°F	mg/dL	%
1	0	45	82	9	0.074
2	0	30	84	4	0.037
3	0	22	84	4	0.037
4	0	30	90	10	0.081
5	0	22	90	5	0.044
6	124	22	92	38	0.318
7	0	45	94	12	0.104
8	124	45	94	63	0.526
9	124	30	95	58	0.481
10	0	45	97	20	0.163
11	0	30	98	16	0.133
12	0	22	95	9	0.074
13	0	45	103	28	0.230

A graph was plotted between I.H and temperature for varying exposure time as shown in Figure 293. The I.H increases from 0.03 % to 0.23 % as the exposure time increases from 20ms to 45ms.

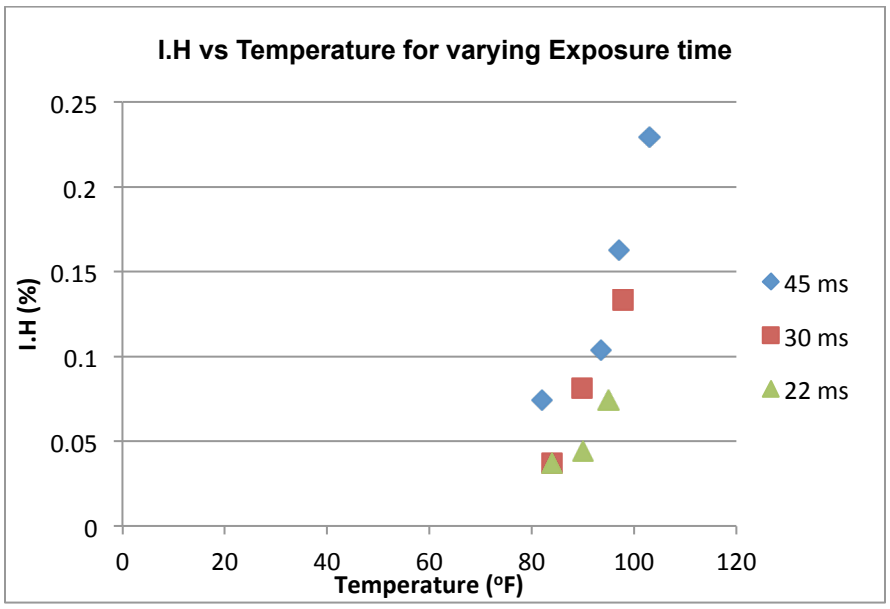

Figure 293: I.H vs Temperature for each sample taken during Trial #2

Using the temperature results obtained, the impact of blood damage due to shear from trial #1 (shown in Table 3) at a particular temperature and exposure time was determined from the difference between the I.H corresponding to the particular shear stress (Trial #1), and I.H of 0 Pa shear stress at that temperature (from Trial #2), and I.H due to aging of blood from 0 Pa obtained before and after the experiment (from Trial #1).

Table 3: I.H (%) only due to shear from Trial #1

Exposure time	Temperature	Blood Damage, I.H (%)					I.H(%) due to shear from Trial #1
		I.H from Trial #1				I.H from Trial #2	
ms	^{o}F	At 124 Pa	At 100 Pa	At 113 Pa	Due to Blood aging	At 0 Pa	
22	92	0.317			0.025	0.058	0.233
22	96		0.208		0.025	0.075	0.108
30	95	0.483			0.025	0.117	0.342
30	94		0.217			0.117	0.1
30	98			0.3		0.133	0.167
45	94	0.525			0.025	0.1	0.4
45	97			0.242		0.167	0.075
45	95		0.300		0.025	0.1	0.175

4 DISCUSSION AND CONCLUSION

This thesis was successful in completing the fabrication of the Maglev shearing device and the analysis for shear damage was carried out. Damage to the blood due to temperature and due to aging in blood was also investigated.

4.1 Working of the Shearing device (Objective 1)

The degree to which blood was damaged was regulated by varying shear stress and exposure time. In the process of investigating the exposure time, it was necessary to know the flow rate of the blood. The syringe pump was capable of supplying consistent flow rate.

In order to determine the shear stress, the factor needed to be taken into account was the speed of the rotor. The speed of the rotor was controlled by the Target system and measured using the HESA signal. The ability to regulate and control the rotor speed and flow rate allowed the device to damage blood.

4.2 Damaging of blood (Objective 2)

The results from the trail #1 show that the relationship between blood damage, shear stress, and exposure time corresponds to that of the hemolysis power law model. According to the hemolysis power law model, blood damage should be exponentially proportional to shear stress and exposure time (Equation 1). Results from trial #1 showed that I.H increased with the increase in shear stress and exposure time, which is the same as that shown in previous studies. Hence, the resultant I.H values obtained were similar to those from previous studies. The results from Trial #1 when compared with Zhang et al results (Figure 5) showed that the I.H values were similar in the range of shear stress and exposure time conducted in this study. Paul et al was not able measure hemolysis damage below 425 Pa shear stress and 620ms exposure time, whereas this study (Trial #1) showed that there was measurable

damage in the shear stress range of 0 to 130 Pa and exposure time range of 20ms to 70ms. However, there wasn't sufficient data to prove the difference in I.H from that of the previous studies. Consequently, the exponential factors obtained were inconsistent to those from previous studies.

The blood damage at 0 Pa for different exposure time showed consistency and minimal damage. However when blood damage was compared between the 0 Pa damage at the start of the trial to the end of the trial (duration of trial 48 hours), there was an I.H increase of 0.025 %. Thus the aging in blood needs to be accounted for in the calculation of shear damage.

As part of the sampling process of Trial #1, the temperature of the inlet and outlet for each sample was recorded (Figure 31). The results showed that there was a measureable increase in temperature upon spinning of the rotor. As such, Trial #2 was carried out to account for the damage due to the temperature. This way, the blood damage could be attributed solely to the temperature and not to shear stress.

The result from the graph (Figure 293) clearly shows that there is a positive correlation between the increase in temperature and increase in I.H After accounting for the blood damage due to temperature and blood damage due to aging (Table 33), it was still observed that the measured I.H values were significantly lower than those of the from the Trial #1. Hence, the results from Trial #1 are conclusive in determining the relationship between blood damage, shear stress, and exposure time (apart from temperature and aging in blood).

4.3 **Future Work**

- Artificial blood cell surrogates can be used for testing instead of a bovine or porcine blood samples. These blood cell surrogates should show actual blood cell properties in order to do

any kind of testing. Since fresh animal blood is not readily available, using it in large amounts for running several tests repeatedly is not practical. Also, the life of the bovine or porcine blood is low; hence all tests need to be conducted within a short period of time. All this could be avoided, if other fluids are used as blood replacements for testing purposes, such as artificial blood surrogates.

- It is observed that temperature of the system had a major impact on the results. In order to gain more confidence in determining the relationship between blood damage, shear stress, and exposure time, further investigation needs to be carried out to understand the extent and effectiveness of temperature in damaging blood and its relationship to shear damage.
- Further work needs to be carried out to collect more data from the device in order to determine a relationship between the I.H obtained from this thesis and previous studies.

5 REFERENCE

1. Paul, R.; Apel, J.; Klaus, S.; Schugner, F.; Schwindke, P.; Reul, H., Shear stress related blood damage in laminar Couette flow. *Artificial Organs* 2003, *27* (6), 517-529.
2. Wu, J. C.; Antaki, J. F.; Snyder, T. A.; Wagner, W. R.; Borovetz, H. S.; Paden, B. E., Design optimization of blood shearing instrument by computational fluid dynamics. *Artificial Organs* 2005, *29* (6), 482-489.
3. Chua, L. P.; Akamatsu, T., Measurements of gap pressure and wall shear stress of a blood pump model. *Medical Engineering & Physics* 2000, *22* (3), 175-188.
4. Zhang, T.; Taskin, M. E.; Fang, H. B.; Pampori, A.; Jarvik, R.; Griffith, B. P.; Wu, Z. J., Study of Flow-Induced Hemolysis Using Novel Couette-Type Blood-Shearing Devices. *Artificial Organs* 2011, *35* (12), 1180-1185.
5. http://www.redcrossblood.org/learn-about-blood/blood-components.
6. Leverett, L. B.; Lynch, E. C.; Alfrey, C. P.; Hellums, J. D., RED BLOOD-CELL DAMAGE BY SHEAR-STRESS. *Biophysical Journal* 1972, *12* (3), 257-&.
7. Chua, L. P.; Song, G. L.; Yu, S. C. M.; Lim, T. M., Computational fluid dynamics of gap flow in a biocentrifugal blood pump. *Artificial Organs* 2005, *29* (8), 620-628.
8. Chua, L. P.; Song, G. L.; Lim, T. M.; Zhou, T. M., Numerical analysis of the inner flow field of a biocentrifugal blood pump. *Artificial Organs* 2006, *30* (6), 467-477.
9. http://anthro.palomar.edu/blood/blood_components.htm, W. P. Blood Components.
10. Farley, A.; Hendry, C.; McLafferty, E., Blood components. *Nursing Standard* 2012, *27* (13), 35-42.
11. http://www.thefreedictionary.com/hemolysis, W. P. Hemolysis Definition.

12. http://www.bupa.co.uk/individuals/health-information/directory/d/deep-vein-thrombosis, W. P., Deep veinThrombosis.
13. Budge Johl, M. L., Reto Schoeb, Effect of a Maglev Centrifugal Pump on Slurry Health and Defect Rates. 2005.
14. StevenW. Day.Magnetically Levitated Implantable Blood Pump.Web. March, 2012.
15. Moser, K. W.; Raguin, L. G.; Harris, A.; Morris, H. D.; Georgiadis, J.; Shannon, M.; Philpott, M., Visualization of Taylor-Couette and spiral Poiseuille flows using a snapshot FLASH spatial tagging sequence. *Magnetic Resonance Imaging* 2000, *18* (2), 199-207.
16. Malinauskas, R. A., Plasma hemoglobin measurement techniques for the in vitro evaluation of blood damage caused by medical devices. *Artificial Organs* 1997, *21* (12), 1255-1267.
17. Cripps, C. M. (1968). Rapid method for the estimation of plasma haemoglobin levels. Journal of Clinical Pathology, 21(1), 110–2.
18. Arnold David Gomez (2009). Control of a magnetically levitated ventricular assist device.
19. O. Myagmar, "Evaluation of CFD based Hemolysis Prediction Methods," August,2011.
20. "http://enerca.org/activities-news/news/18/eculizumab-reduces-paroxysmal-nocturnal-hemoglobinuria-complications-and-improves-survival". Web. March, 2013.
21. "https://www.boundless.com/physiology/textbooks/boundless-anatomy-and-physiology-textbook/blood-17/erythrocytes-red-blood-cells-165/rbc-anatomy-828-2192". Web. April, 2013.
22. "http://www.bupa.com.au/health-and-wellness/health-information/az-health-information/deep-vein-thrombosis". Web. March, 2012.
23. "http://leavingbio.net/blood.htm". Web. March, 2012.
24. "http://www.fda.gov/MedicalDevices/DeviceRegulationandGuidance/GuidanceDocuments/ucm073668.htm". Web, December, 2014

25. W.M. Allcroft. Observation on the hemoglobin levels of cows and sheep. Web. December, 2014.

A APPENDIX A

A.1 Bread Board Connection

All the active components are powered, controlled, and displayed through the target system, hence the wiring from these components are connected to the target system through the bread board (shown in Table A-1).

Table A-1: Color coding of the wires from and to the bread board

COLOR CODING OF THE WIRES										
FROM SHEARING DEVICE				PCB Pin	AMB & MOTOR	PCB Pin	TO XPC TARGET			
Wire 2		Wire 1					Wire 1		Wire 2	
Wire	Band	Wire	Band				Wire	Band	Wire	Band
		BLACK		11	PHC	11	BLACK			
		WHITE		10	PHB	10	WHITE			
		RED		9	PHA	9	RED			
		BLUE		8	RYN	8	YELLOW	BROWN		
		PINK		7	RYP	7	BROWN	WHITE	ORANGE	BROWN
		GRAY		6	RXN	6	BROWN	YELLOW	YELLOW	BROWN
		VIOLET		5	RXP	5	BROWN	ORANGE	WHITE	BROWN
		BROWN		4	FYN	4	BROWN	TAN		
		GREEN		3	FYP	3	TAN	WHITE	TAN	BROWN
		ORANGE		2	FXN	2	TAN	BROWN		
		YELLOW		1	FXP	1	BROWN	PINK	WHITE	TAN
					HESA					
ORANGE		ORANGE		1	5V	1	WHITE	PINK	WHITE	ORANGE
BROWN		BROWN		2	GND	2	PINK	WHITE	TAN	ORANGE
		RED		3	H_{FXP}	3	TAN	VIOLET	WHITE	VIOLET
		YELLOW		4	H_{FYP}	4	WHITE	GRAY	TAN	GRAY

		GREEN		5	H_{FXN}	5	VIOLET	WHITE	VIOLET	TAN
		BLACK		6	H_{FYN}	6	GRAY	WHITE	GRAY	TAN
		RED		7	H_{RXP}	7	WHITE	GREEN	TAN	GREEN
		GREEN		8	H_{RXN}	8	GREEN	WHITE	GREEN	TAN
		YELLOW		9	H_{RYP}	9	WHITE	BLUE	TAN	BLUE
		BLACK		10	H_{RYN}	10	BLUE	WHITE	BLUE	TAN

A.2 Run out Testing

During the spinning of the rotor at different speeds, the rotor might revolve in an orbit reducing the region 1 much less and this might cause additional damage to the blood. Hence it is essential to determine the distance of the gap region (region 1) during spinning of the rotor.

In order to determine the run out displacement of the rotor, an AR700 Acuity Displacement laser is used as described in this section.

A.2.1 Specifications

Acuity AR700 Displacement Sensor

Model : - 0125

Power : 15 – 24 Volt DC, 120 – 200 mA

Analog Output : 4-20 MA or 0- 10 V

Two parameters were to be calibrated before the run out displacement could be measure which was the Frequency and the Amplitude.

A.2.2 Calibration of the Acuity AR700 laser

a. **Frequency Calibration**

Frequency of the laser sampling rate is calibrated by using the laser to determine the displacement of a linear actuator of known frequency. The laser is then connected an O- scope to determine the frequency (shown in Figure A-1).

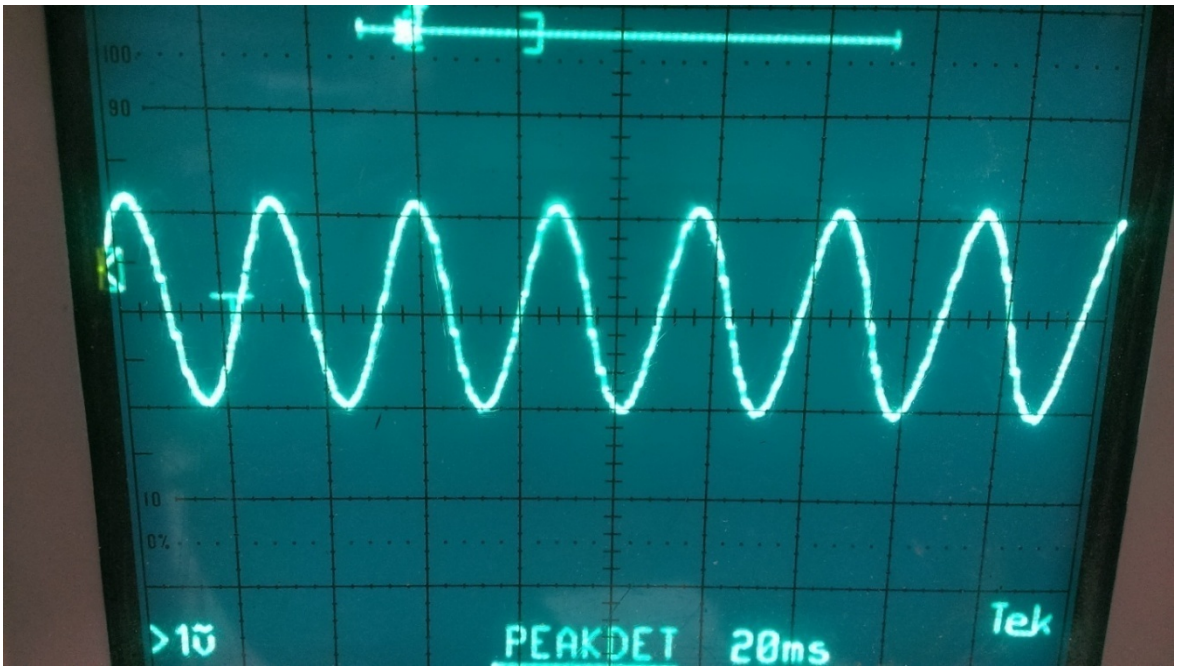

Figure

A-1: Sine wave formation in an oscilloscope for the Acuity laser

The above O-scope reading is for 35 Hz linear displacement motion

From the Wave, Time for 5 oscillation = 144ms = .144 sec

Hence Frequency for 1 oscillation = $\left(\left(\frac{1}{0.144}\right) * 5\right)$

$= 34.7 \sim 35$ Hz

This in turn proves the frequency of the Linear Displacement

b. **Amplitude**

To determine the amplitude, the laser is setup on a table with the laser point facing the tip of a Vernier caliper jaw. This way, as the Vernier caliper jaw moves further from the laser, the voltage keeps increasing. Ten readings were taken by repeating the experiment ten times (Table A-2) and using these readings the relation between voltage and actual distance was determined (Figure A-2).

Table A-2: Readings obtained from the Acuity laser AR700

minimum detectable distance from the laser (mm)			11.04			
maximum detectable distance from the laser (mm)			14.33			
Vernier Caliper (mm)			V.C Reading	Multimeter	Ratio	Average
V.C reading 1	V.C reading 2	Difference	Laser Range	Voltage (v)	V/mm	
24.35	12.89	11.46	0.42	1.63	3.8809524	3.165218
24.35	12.67	11.68	0.64	2.39	3.734375	
24.35	12.4	11.95	0.91	3.16	3.4725275	
24.35	12.04	12.31	1.27	3.94	3.1023622	
24.35	11.79	12.56	1.52	4.606	3.0302632	
24.35	11.72	12.63	1.59	5	3.1446541	
24.35	10.95	13.4	2.36	7.46	3.1610169	
24.35	10.86	13.49	2.45	7.79	3.1795918	
24.35	10.65	13.7	2.66	8.44	3.1729323	
24.35	10.48	13.87	2.83	8.95	3.1625442	
24.35	10.32	14.03	2.99	9.48	3.1705686	

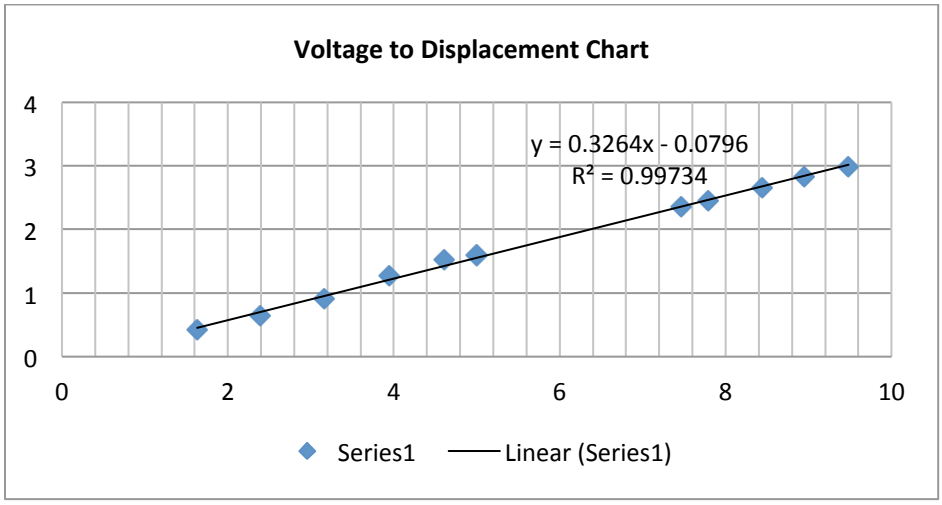

Figure A-2: Graph for Voltage to Displacement Chart obtained for the AR700 displacement laser

Thus 1 mm = 3.0637 V

A.2.3 To determine the Run out of the rotor

The run out of the rotor is to be determined for both front and the rear and is done by setting the laser to face the front and the rear separately. The spinning of the rotor at its minimum speed is 2000rpm which is equivalent to 35 Hz in frequency. Hence the sampling is set at a safe frequency of 2000 Hz.

The laser reading during spinning is noted by facing it to the tips of the rotor and two distinct numbers are obtained. These two numbers are subtracted from one another to obtain the slant height (S) (shown in Figure A-3). Using basic trigonometry, the actual length M is determined. This displacement M is the run out distance of the rotor during spinning.

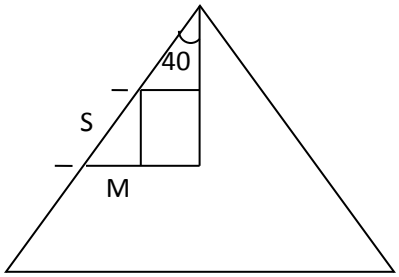

Figure A-3: Cone formation of the rotor at the either ends

a. **Front**

The laser is pointed at the slant height of the conical part of the rotor as shown in the Figure A-4.

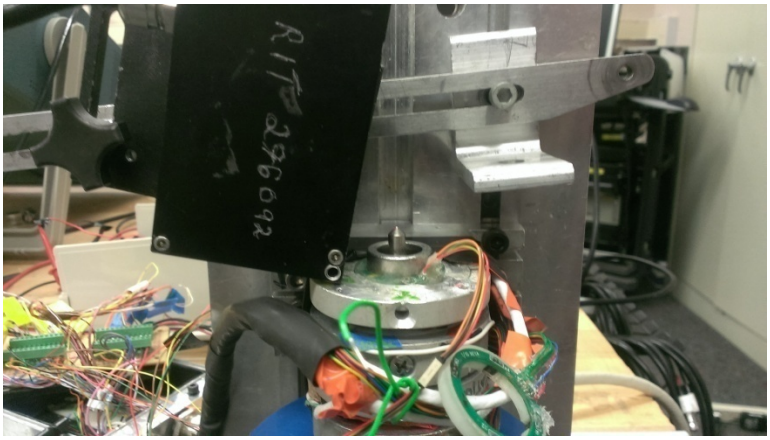

Figure A-4: Position of the l

aser at the front of the shearing device

Laser Readings during levitation - 8.45V

Laser reading during spinning (Range) - 8.145V to 8.17V

Distance to voltage conversion: 1 mm = 3.0627 V

Hence the range in distance =$\left(\frac{8.145}{3.0627}\right)$to $\left(\frac{8.7}{3.0627}\right)$

= 2.506 mm to 2.5138 mm

Thus the Run out Slant distance (S) = 2.506 mm - 2.5138 mm

= 0.01 mm

Finally actual Distance M = Sin 40 * S

= 0.006mm

This can be considered that at 2000 rpm spindle rotation in air, the run out of the rear of the rotor is 0.006mm.

b. **Rear**

The laser is pointed at the slant height of the conical part of the rotor as shown in the Figure A-5.

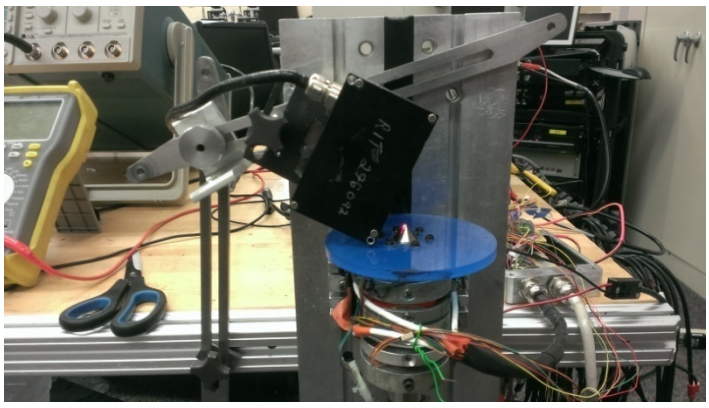

Figure A-5: Position of the laser at the rear of the shearing device

Laser Readings during levitation - 7.9V

Laser reading during spinning (Range) - 7.88V to 7.914V

Repeating the same calculation process the actual distance M = 0.01 mm.

Hence 0.01 mm and 0.006mm of the front and the rear of the rotor run out respectively will not matter much compared 0.23mm, which is the gap height.

A.3 Initial Testing and Performance

The sensors responsiveness and polarity in the front and the rear needs be checked and the center of the housing was determined for a successful levitation and spinning. They can be determined by Matlab programs of AutoHESA and Centering Program respectively.

A.3.1 AutoHESA

The AutoHESA program is programmed to make the rotor oscillate at four positions in the order of right left up and down inside the housing cylinder. The Figure A-6 illustrates the rotor oscillations at each point. The polarity of the rotor was adjusted in such a way that it coordinates to a sequence.

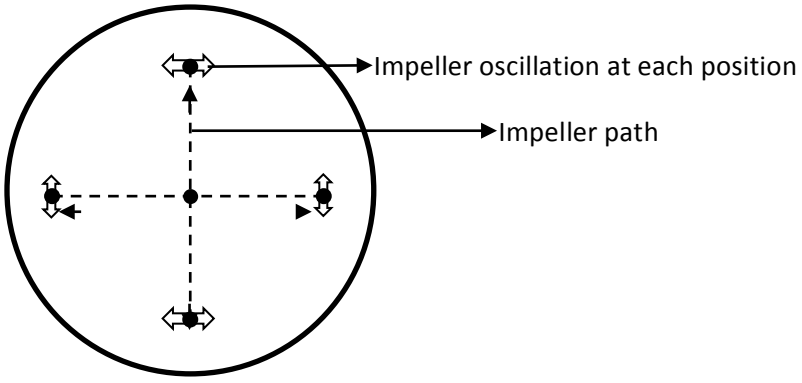

FigureA-6: Movement of rotor for the AUTO HESA program

A.3.2 Centering

The magnetic center of the rotor is required for a successful levitation and spinning. The center would vary if the sensors were moved or if the housing is moved overall. An appropriate center can be determined using the Matlab program and also by manual movement of the rotor during levitation and spinning separately.

The coding for the centering program in Matlab is such that the rotor is made to spin inside the housing, thus giving the center of the spinning orbit. The center is given in the form of 8 voltages.

The center can be determined physically for spinning and levitation by changing these voltages manually in each direction while moving the rotor from one side to another during spinning and levitation respectively.

The conversion from voltage to distance (From Simulink coding)

$$1V=0.002m$$

A.4 Preliminary Blood test

The preliminary blood measurement test was conducted in order to understand the procedure and trial for the betterment of the actual blood damage measurement. During the course of this study, it was observed that the heat of the device was elevating. Hence a cooling fan was adjacent to the device and a heat exchanging system was implemented to the base of the shearing device. The heat exchanger utilized tap water as the coolant (shown in the Figure A-7).

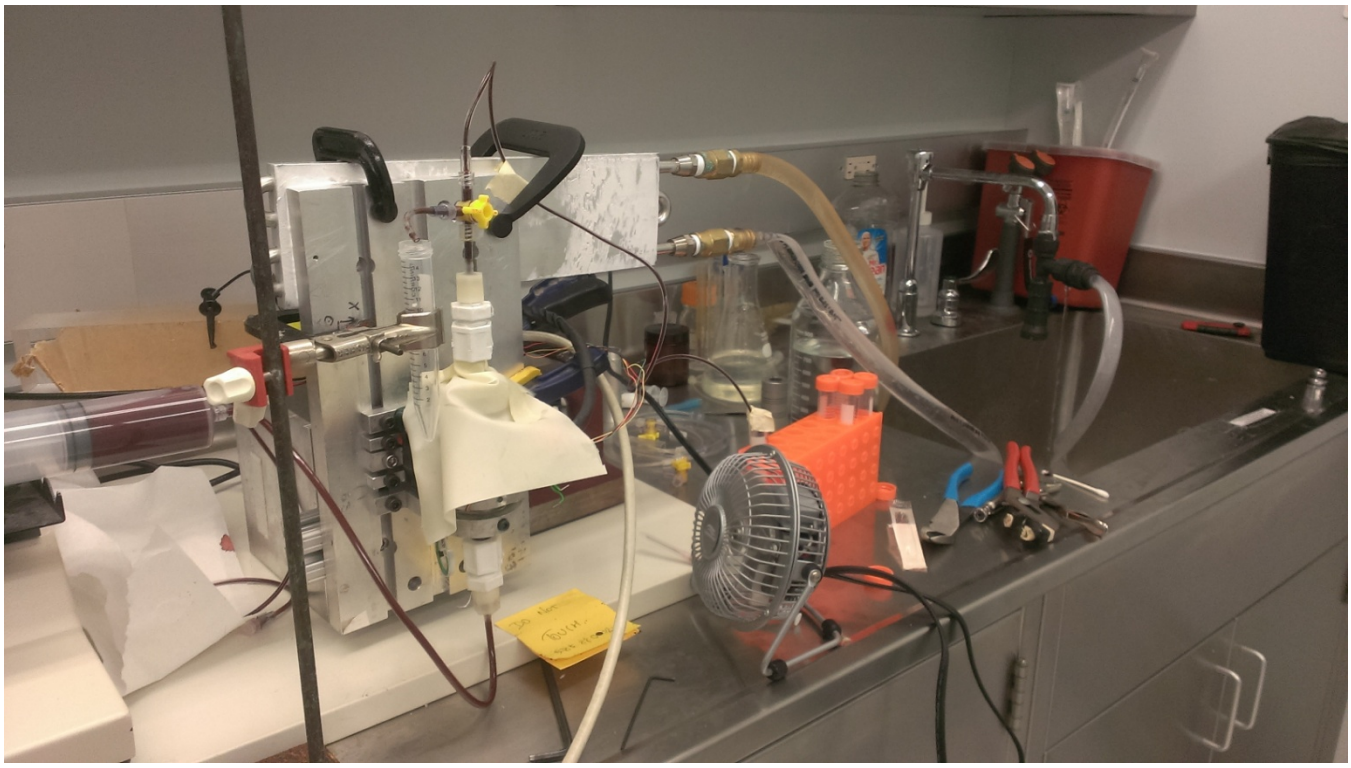

Figure A-7: Set up of the blood shearing experiment Trial #1

A.4.1 Result and Discussion

The Index of Hemolysis for different shear stress and exposure time are determined during the study and are recorded in the Table A-3.

Table A-3: Measured Index of Hemolysis (I.H) at varying levels of shear stress and exposure time during Trial#1

Sample #	SHEAR STRESS	EXPOSURE TIME	fHb	I.H
	Pa	ms	mg/dL	%
1	124	30	47	0.392
2	68	30	49	0.408
3	90	30	32	0.267
4	68	67	94	0.783
5	68	45	76	0.633
6	144	30	60	0.5
7	144	22	76	0.633
8	90	67	55	0.458
9	124	22	38	0.317
10	124	22	43	0.358
11	124	45	51	0.425
12	124	45	59	0.492
13	124	67	83	0.692
14	124	67	115	0.958
15	66	22	42	0.35
16	90	22	28	0.233
17	90	45	41	0.342
18	0	6.7	52	0.433

A graph was plotted between I.H and exposure time for varying shear stress as shown in Figure A-8. The I.H increases from 0.3 % to 1 % as the exposure time increases from 20ms to 70ms. The curves were drawn between the I.H and exposure time for varying shear stress by the experimental data acquired during the blood test. All the experiments in this trial were conducted in the time period of 48 hours.

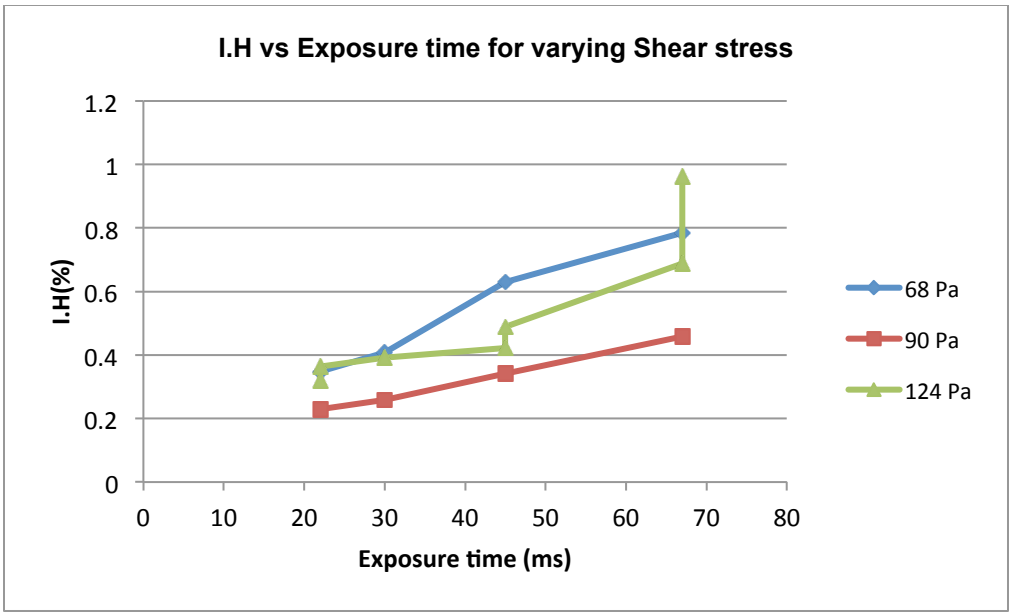

Figure A-8: I.H vs Exposure time for varying shear stress

A graph was also plotted between I.H and shear stress for varying exposure time as shown in Figure A-9. The I.H decreased from 0.8 % to 0.2 % before increasing from 0.2 % to 1 % as the shear stress increases from 60 Pa to 150 Pa. The curves were drawn between the I.H and exposure time for varying shear stress by the experimental data acquired during the blood test.

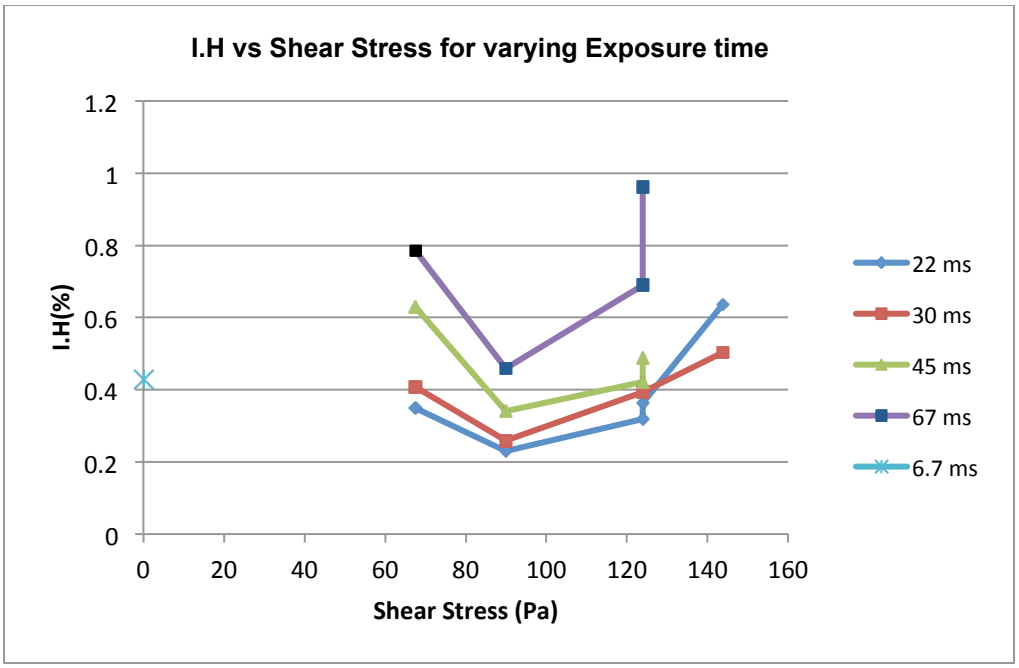

Figure A-9: I.H vs Shear stress for varying exposure time

The results from the graph of I.H vs Exposure time from the preliminary trial (Figure A-8) show that the Index of Hemolysis does vary with respect to exposure time. The results from the graph of I.H vs Shear stress from the same trial (Figure A-9) shows that the hemolysis damage initially decreases before increasing. The initial trial (Trial #1) yielded unusual results due to improper operational procedures, such as lack of proper device cleaning protocols, mismeasurement of dump time, etc. No data was taken for 0 Pa (no rotor rotation) shear stress during this trial to determine a distinct pattern in the results. During the course of trial, it was observed that the surface temperature of the device was elevating. All these factors were accounted for during the actual blood testing (Trial #1 and Trial #2).